Jurassic NLR: conserved and dynamic evolutionary features of the atypically ancient immune receptor ZAR1

Hiroaki Adachi[1,2,3], Toshiyuki Sakai[1,2], Jiorgos Kourelis[1], Hsuan Pai[1], Jose L. Gonzalez Hernandez[4], Yoshinori Utsumi[5], Motoaki Seki[5,6,7], Abbas Maqbool[1] and Sophien Kamoun[1*]

[1]The Sainsbury Laboratory, University of East Anglia, Norwich Research Park, NR4 7UH, Norwich, UK

[2]Laboratory of Crop Evolution, Graduate School of Agriculture, Kyoto University, Mozume, Muko, Kyoto 617-0001, Japan

[3]JST-PRESTO, Saitama, Japan

[4]Agronomy, Horticulture and Plant Sciences Department, South Dakota State University, Brookings, South Dakota, US

[5]Plant Genomic Network Research Team, RIKEN Center for Sustainable Resource Science, 1-7-22 Suehiro-cho, Tsurumi-ku, Yokohama, Kanagawa 230-0045, Japan

[6]Plant Epigenome Regulation Laboratory, RIKEN Cluster for Pioneering Research, 2-1 Hirosawa, Wako, Saitama 351-0198, Japan

[7]Kihara Institute for Biological Research, Yokohama City University, 641-12 Maioka-cho, Totsuka-ku, Yokohama, Kanagawa 244-0813, Japan

*For correspondence: sophien.kamoun@tsl.ac.uk

Short title: Evolution of ZAR1 since the Jurassic era

The author responsible for distribution of materials integral to the findings presented in this article in accordance with the policy described in the Instructions for Authors (https://academic.oup.com/plcell/pages/General-Instructions) is: Sophien Kamoun (sophien.kamoun@tsl.ac.uk)."

ABSTRACT

In plants, NLR immune receptors generally exhibit hallmarks of rapid evolution even at the intraspecific level. We used iterative sequence similarity searches coupled with phylogenetic analyses to reconstruct the evolutionary history of ZAR1, an atypically conserved NLR that traces its origin to early flowering plant lineages ~220 to 150 million years ago (Jurassic period). We discovered 120 ZAR1 orthologs in 88 species, including the monocot *Colacasia esculenta*, the magnoliid *Cinnamomum micranthum* and the majority of eudicots, notably the early diverging eudicot species *Aquilegia coerulea*. Ortholog sequence analyses revealed highly conserved features of ZAR1, including regions for pathogen effector recognition and cell death activation. We functionally reconstructed the cell death activity of ZAR1 and its partner receptor-like cytoplasmic kinase (RLCK) from distantly related plant species, experimentally validating the hypothesis that ZAR1 has evolved to partner with RLCKs early in its

evolution. In addition, ZAR1 acquired novel molecular features. In cassava and cotton, ZAR1 carries a C-terminal integration of a thioredoxin-like domain, and in several taxa, ZAR1 duplicated into two paralog families, which underwent distinct evolutionary paths. We conclude that ZAR1 stands out among angiosperm NLRs for having experienced relatively limited gene duplication and expansion throughout its deep evolutionary history. Nonetheless, ZAR1 did also give rise to non-canonical NLR proteins with integrated domains and degenerated molecular features.

IN A NUTSHELL

Background: In plants, nucleotide-binding leucine-rich repeat (NLR) immune receptors generally exhibit hallmarks of rapid evolution even at the intraspecific level. NLRs evolve primarily through the birth-and-death process: new NLRs emerge by recurrent cycles of gene duplication and loss—some genes are maintained in the genome acquiring new pathogen detection specificities, whereas others are deleted or become non-functional through the accumulation of deleterious mutations. Such dynamic patterns of evolution enable the NLR immune system to keep up with fast-evolving effector repertoires of pathogenic microbes. However, unlike typical NLRs, ZAR1 (HOPZ-ACTIVATED RESISTANCE1) is conserved across angiosperms.

Question: Can we use a molecular evolution framework to determine the critical features of a conserved plant NLRs?

Findings: We performed iterative sequence similarity searches coupled with phylogenetic analyses to reconstruct the evolutionary history of ZAR1. ZAR1 is

an atypically conserved NLR that traces its origin to early flowering plant lineages ~220 to 150 million years ago (Jurassic period). Ortholog sequence analyses revealed highly conserved features of ZAR1, including regions for pathogen recognition and immune activation. We functionally reconstructed the immune activity of ZAR1 and its host partner receptor-like cytoplasmic kinases (RLCKs) from distantly related plant species, supporting the hypothesis that ZAR1 has evolved to partner with RLCKs early in its evolution. ZAR1 stands out among angiosperm NLRs for having experienced relatively limited gene duplication and expansion throughout its deep evolutionary history.

Next steps: Further comparative analyses, combining molecular evolution and structural biology, of plant and animal NLR systems will yield novel experimentally testable hypotheses for NLR research.

INTRODUCTION

Plant immune receptors, often encoded by disease resistance (*R*) genes, detect invading pathogens and activate innate immune responses that can limit infection (Jones and Dangl, 2006). A major class of immune receptors is formed by intracellular proteins of the nucleotide-binding leucine-rich repeat (NLR) family (Dodds and Rathjen, 2010; Jones et al., 2016; Kourelis and van der Hoorn, 2018). NLRs detect host-translocated pathogen effectors either by directly binding them or indirectly via host proteins known as guardees or decoys. NLRs are arguably the most diverse protein family in flowering plants (angiosperms) with many species having large (>100) and diverse repertoires of NLRs in their genomes (Shao et al., 2016; Baggs et al., 2017; Kourelis et al., 2021). They

typically exhibit hallmarks of rapid evolution even at the intraspecific level (Van de Weyer et al., 2019; Lee and Chae, 2020; Prigozhin and Krasileva, 2020). Towards the end of the 20th century, Michelmore and Meyers (1998) proposed that NLRs evolve primarily through the birth-and-death process. In this model, new NLRs emerge by recurrent cycles of gene duplication and loss—some genes are maintained in the genome acquiring new pathogen detection specificities, whereas others are deleted or become non-functional through the accumulation of deleterious mutations. Such dynamic patterns of evolution enable the NLR immune system to keep up with fast-evolving effector repertoires of pathogenic microbes. However, as already noted over 20 years ago by Michelmore and Meyers (1998), a subset of NLR proteins are slow evolving and have remained fairly conserved throughout evolutionary time (Wu et al., 2017; Stam et al., 2019). These “high-fidelity” NLRs (per Lee and Chae, 2020) offer unique opportunities for comparative analyses, providing a molecular evolution framework to reconstruct key transitions and reveal functionally critical biochemical features (Delaux et al., 2019). Nonetheless, comprehensive evolutionary reconstructions of conserved NLR proteins remain limited despite the availability of a large number of plant genomes across the breadth of plant phylogeny. One of the reasons is that the great majority of NLRs lack clear-cut orthologs across divergent plant taxa. Here, we address this gap in knowledge by investigating the macroevolution of ZAR1 (HOPZ-ACTIVATED RESISTANCE1), an atypically ancient NLR, and asking fundamental questions about the conservation and diversification of this immune receptor throughout its deep evolutionary history.

NLRs generally function in non-self perception and innate immunity in plants and animals (Jones et al., 2016; Uehling et al., 2017). In the broadest biochemical definition, plant NLRs share a multidomain architecture typically consisting of a NB-ARC (nucleotide-binding domain shared with APAF-1, various R-proteins and CED-4) followed by a leucine- rich repeat (LRR) domain. Angiosperm NLRs form several major monophyletic groups with distinct N-terminal domain fusions (Shao et al., 2016; Kourelis et al., 2021). These include the subclades TIR-NLR with the Toll/interleukin-1 receptor (TIR) domain, CC-NLR with the Rx-type coiled-coil (CC) domain, CC_R-NLR with the RPW8-type CC (CC_R) domain (Tamborski and Krasileva, 2020) and the more recently defined CC_{G10}-NLR with a distinct type of CC (CC_{G10}) (Lee et al., 2020). Up to 10% of NLRs carry unconventional “integrated” domains in addition to the canonical tripartite domain architecture. Integrated domains are thought to generally function as decoys to bait pathogen effectors and enable pathogen detection (Cesari et al., 2014; Sarris et al., 2016; Wu et al., 2015; Kourelis and van der Hoorn, 2018). They include dozens of different modules indicating that novel domain acquisitions have repeatedly taken place throughout the evolution of plant NLRs (Sarris et al., 2016; Kroj et al., 2016). To date, over 400 NLRs from 31 genera in 11 orders of flowering plants have been experimentally validated as reported in the RefPlantNLR reference dataset (Kourelis et al., 2021). Several of these NLRs are coded by *R* genes that function against economically important pathogens and contribute to sustainable agriculture (Dangl et al., 2013).

In recent years, the research community has gained a better understanding of the structure/function relationships of plant NLRs and the immune receptor circuitry they form (Wu et al., 2018; Adachi et al., 2019a; Burdett et al., 2019; Jubic et al., 2019; Bayless and Nishimura, 2020; Feehan et al., 2020; Mermigka et al., 2020; Wang and Chai, 2020; Xiong et al., 2020; Zhou and Zhang, 2020). Some NLRs, such as ZAR1, form a single functional unit that carries both pathogen sensing and immune signalling activities in a single protein (termed 'singleton NLR' per Adachi et al., 2019a). Other NLRs function together in pairs or more complex networks, where connected NLRs have functionally specialized into sensor NLRs dedicated to pathogen detection or helper NLRs that are required for sensor NLRs to initiate immune signalling (Feehan et al., 2020). Paired and networked NLRs are thought to have evolved from multifunctional ancestral receptors through asymmetrical evolution (Adachi et al., 2019a; 2019b). As a result of their direct coevolution with pathogens, NLR sensors tend to diversify faster than helpers and can be dramatically expanded in some plant taxa (Wu et al., 2017; Stam et al., 2019). For instance, sensor NLRs often exhibit non-canonical biochemical features, such as degenerated functional motifs and unconventional domain integrations (Adachi et al., 2019b; Seong et al., 2020).

The elucidation of plant NLR structures by cryo-electron microscopy has significantly advanced our understanding of the biochemical events associated with the activation of these immune receptors (Wang et al., 2019a; 2019b; Ma et al., 2020; Martin et al., 2020). The CC-NLR ZAR1, the TIR-NLRs RPP1 and Roq1 oligomerize upon activation into a multimeric complex known as the

169 resistosome. In the case of ZAR1, recognition of bacterial effectors occurs
170 through its partner receptor-like cytoplasmic kinases (RLCKs), which occur in a
171 genomic cluster of multiple RLCK-type pseudokinases that vary depending on
172 the pathogen effector and host plant (Lewis et al., 2013; Wang et al., 2015; Seto
173 et al., 2017; Schultink et al. 2019; Laflamme et al., 2020). Activation of ZAR1
174 induces conformational changes in the nucleotide binding domain resulting in
175 ADP release, dATP/ATP binding and pentamerization of the ZAR1–RLCK
176 complex into the resistosome. The ZAR1 resistosome exposes a funnel-shaped
177 structure formed by the N-terminal α1 helices, which translocates into the
178 plasma membrane, and the resistosome itself acts as a Ca^{2+} channel (Wang et
179 al., 2019b; Bi et al., 2021). The ZAR1 N-terminal α1 helix matches the MADA
180 consensus sequence motif that is functionally conserved in ~20% of CC-NLRs
181 including NLRs from dicot and monocot plant species (Adachi et al., 2019b).
182 This suggests that the biochemical 'death switch' mechanism of the ZAR1
183 resistosome may apply to a significant fraction of CC-NLRs. Interestingly, unlike
184 singleton and helper CC-NLRs, sensor CC-NLRs often carry degenerated MADA
185 α1 helix motifs and/or N-terminal domain integrations, which would preclude
186 their capacity to trigger cell death according to the ZAR1 model (Adachi et al.,
187 2019b; Seong et al., 2020).
188
189 Comparative sequence analyses based on a robust evolutionary framework can
190 yield insights into molecular mechanisms and help generate experimentally
191 testable hypotheses. ZAR1 was previously reported to be conserved across
192 multiple dicot plant species but whether it occurs in other angiosperms hasn't

been systematically studied (Lewis et al., 2010; Baudin et al., 2017; Schultink et al., 2019; Harant et al., 2022). Here, we used a phylogenomic approach to investigate the molecular evolution of ZAR1 across flowering plants (angiosperms). We discovered 120 ZAR1 orthologs in 88 species, including monocot, magnoliid and eudicot species indicating that ZAR1 is an atypically conserved CC-NLR that traces its origin to early angiosperm lineages ~220 to 150 million years ago (Jurassic period). We took advantage of this large collection of orthologs to identify highly conserved features of ZAR1, revealing regions for effector recognition, intramolecular interactions and cell death activation. We showed that the cell death activity of ZAR1 from distantly related plant species can be dependent of its partner RLCKs, therefore experimentally validating the hypothesis that ZAR1 has evolved to be a partner with RLCKs early in its evolution. Throughout its evolution, ZAR1 also acquired novel features, including the C-terminal integration of a thioredoxin-like domain and duplication into two paralog families ZAR1-SUB and ZAR1-CIN. Members of the ZAR1-SUB paralog family have highly diversified in eudicots and often lack conserved ZAR1 features. We conclude that ZAR1 has experienced relatively limited gene duplication and expansion throughout its deep evolutionary history, but still did give rise to non-canonical NLR proteins with integrated domains and degenerated molecular features.

RESULTS

ZAR1 is the most widely conserved CC-NLR across angiosperms

To determine the distribution of ZAR1 across plant species, we applied a computational pipeline based on iterated BLAST searches of plant genome and protein databases (Figure 1A). These comprehensive searches were seeded with previously identified ZAR1 sequences from Arabidopsis, *N. benthamiana*, tomato, sugar beet and cassava (Baudin et al., 2017; Schultink et al., 2019; Harant et al., 2022). We also performed iterated phylogenetic analyses using the NB-ARC domain of the harvested ZAR1-like sequences, and obtained a well-supported clade that includes the previously reported ZAR1 sequences, as well as new clade members from more distantly related plant species, notably *Colacasia esculenta* (taro, Alismatales), *Cinnamomum micranthum* (Syn. *C. kanehirae*, stout camphor, Magnoliidae) and *Aquilegia coerulea* (columbine, Ranunculales) (Supplemental Data Set 1). In total, we identified 120 ZAR1 from 88 angiosperm species that tightly clustered in the ZAR1 phylogenetic clade (Figure 1B, Supplemental Data Set 1). Among the 120 genes, 108 code for canonical CC-NLR proteins with 52.0 to 97.0% similarity to Arabidopsis ZAR1, whereas another 9 carry the three major domains of CC-NLR proteins but have a C-terminal integrated domain (ZAR1-ID, see below). The remaining 3 genes code for two truncated NLRs and a potentially mis-annotated coding sequence due to a gap in the genome sequence. In summary, we propose that the identified clade consists of ZAR1 orthologs from a diversity of angiosperm species. Our analyses of ZAR1-like sequences also revealed two well-supported sister clades of the ZAR1 ortholog clade (Figure 1B). We named these subclades ZAR1-SUB and ZAR1-CIN [referred to as ZAR1-sis and ZAR1-basal in Gong et al. (2022),

respectively] and we describe them in more details below.

We have recently proposed that ZAR1 is the most conserved CC-NLR between rosid and asterid plants (Harant et al., 2022). To further evaluate ZAR1 conservation relative to other CC-NLRs across angiosperms, we used a phylogenetic tree of 1475 NLRs from the monocot taro, the magnoliid stout camphor and 6 eudicot species (columbine, Arabidopsis, cassava, sugar beet, tomato, *N. benthamiana*) to calculate the phylogenetic (patristic) distance between each of the 49 Arabidopsis CC-NLRs and their closest neighbor from each of the other plant species. As shown in Harant et al. (2022), ZAR1 stands out for having the shortest phylogenetic distance to its orthologs relative to other CC-NLRs in this diverse angiosperm species set (Supplemental Figure 1). A similar analysis where we plotted the phylogenetic distance between each of the 159 *N. benthamiana* CC-NLRs to their closest neighbor from the other species also revealed ZAR1 as displaying the shortest patristic distance across all examined species (Supplemental Figure 2). These analyses revealed that ZAR1 is possibly the most widely conserved CC-NLR in flowering plants (angiosperms).

Phylogenetic distribution of ZAR1 in angiosperms

Although ZAR1 is distributed across a wide range of angiosperms, we noted particular patterns in its phylogenetic distribution. Supplemental Data Set 1 describes the gene identifiers and other features of ZAR1 orthologs sorted based on the phylogenetic clades reported by Smith and Brown (2018). 68 of the 88

plant species have a single-copy of ZAR1 whereas 20 species have two or more copies (Supplemental Data Set 2). ZAR1 is primarily a eudicot gene but we identified three ZAR1 orthologs outside the eudicots, two in the monocot taro and another one in the magnoliid stout camphor. We failed to detect ZAR1 orthologs in 39 species among the 127 species we examined (Supplemental Data Set 1). Except for taro, ZAR1 is missing in monocot species (17 examined), including in the well-studied *Hordeum vulgare* (barley), *Oryza sativa* (rice), *Triticum aestivum* (wheat) and *Zea mays* (maize). ZAR1 is also missing in all examined species of the eudicot Fabales, Cucurbitales, Apiales and Asterales. However, we found a ZAR1 ortholog in the early diverging eudicot columbine and ZAR1 is widespread in other eudicots, including in 63 rosid, 4 Caryophyllales and 18 asterid species.

ZAR1 is an ancient Jurassic gene that predates the split between monocots, magnoliids and eudicots

The overall conservation of the 120 ZAR1 orthologs enabled us to perform phylogenetic analyses using the full-length protein sequence and not just the NB-ARC domain as generally done with NLRs (Figure 2, Supplemental Figure 3). These analyses yielded a robust ZAR1 phylogenetic tree with well-supported branches that generally mirrored established phylogenetic relationships between the examined plant species (Smith and Brown, 2018; Chaw et al., 2019). For example, the ZAR1 tree matched a previously published species tree of angiosperms based on 211 single-copy core ortholog genes (Chaw et al., 2019). We conclude that the origin of the ZAR1 gene predates the split between

monocots, magnoliids and eudicots and its evolution traced species divergence ever since. We postulate that ZAR1 probably emerged in the Jurassic era ~220 to 150 million years ago (Mya) based on the species divergence time estimate of Chaw et al. (2019) and consistent with the latest fossil evidence for the emergence of flowering plants (Fu et al., 2018; Cui et al., 2022).

ZAR1 is a genetic singleton in a locus that exhibits gene co-linearity across eudicot species

NLR genes are often clustered in loci that are thought to accelerate sequence diversification and evolution (Michelmore and Meyers, 1998; Lee and Chae, 2020). We examined the genetic context of ZAR1 genes using available genome assemblies of taro, stout camphor, columbine, Arabidopsis, cassava, sugar beet, tomato and *N. benthamiana*. The ZAR1 locus is generally devoid of other NLR genes as the closest NLR is found in the Arabidopsis genome 183 kb away from ZAR1 (Supplemental Data Set 3). We conclude that ZAR1 has probably remained a genetic singleton NLR gene throughout its evolutionary history in angiosperms.

Next, we examined the ZAR1 locus for gene co-linearity across the examined species. We noted a limited degree of gene co-linearity between Arabidopsis vs. cassava, cassava vs. tomato, and tomato vs. *N. benthamiana* (Supplemental Figure 4). Flanking conserved genes include the ATPase and protein kinase genes that are present at the ZAR1 locus in both rosid and asterid eudicots. In

contrast, we didn't observe conserved gene blocks at the ZAR1 locus of taro, stout camphor and columbine, indicating that this locus is divergent in these species. Overall, although limited, the observed gene co-linearity in eudicots is consistent with the conclusion that ZAR1 is a genetic singleton with an ancient origin.

ZAR1 orthologs carry sequence motifs known to be required for Arabidopsis ZAR1 resistosome function

The overall sequence conservation and deep evolutionary origin of ZAR1 orthologs combined with the detailed knowledge of ZAR1 structure and function provide a unique opportunity to explore the evolutionary dynamics of this ancient immune receptor in a manner that cannot be applied to more rapidly evolving NLRs. We used MEME (Multiple EM for Motif Elicitation) (Bailey and Elkan, 1994) to search for conserved sequence patterns among the 117 ZAR1 orthologs (ZAR1 and ZAR1-ID) that encode full-length CC-NLR proteins. This analysis revealed several conserved sequence motifs that span across the ZAR1 orthologs (range of protein lengths: 753-1132 amino acids) (Figure 3A, Supplemental table 1). In Figure 3A, we described the major five sequence motifs or interfaces known to be required for Arabidopsis ZAR1 function that are conserved across ZAR1 orthologs.

Effector recognition by ZAR1 occurs indirectly via binding to RLCKs through the LRR domain. Key residues in the Arabidopsis ZAR1-RLCK interfaces are highly

conserved among ZAR1 orthologs and were identified by MEME as conserved sequence patterns (Figure 3A). Valine (V) 544, histidine (H) 597, glycine (G) 645, proline (P) 816, tryptophan (W) 825 and phenylalanine (F) 839 in the Arabidopsis ZAR1 LRR domain were validated by mutagenesis as important residues for RLCK binding whereas isoleucine (I) 600 was not essential (Wang et al., 2015; Baudin et al., 2017; Wang et al., 2019a; Hu et al., 2020). In the 117 ZAR1 orthologs, V544, H597, G645, P816, W825 and F839 are conserved in 88-100% of the proteins compared to only 63% for I600.

After effector recognition, Arabidopsis ZAR1 undergoes conformational changes from monomeric inactive form to oligomeric active state. This is mediated by ADP release from the NB-ARC domain and subsequent ATP binding, which triggers further structural remodelling in ZAR1 leading to the formation of the activated pentameric resistosome (Wang et al., 2019b). NB-ARC sequences that coordinate binding and hydrolysis of dATP, namely P-loop and MHD motifs, are highly conserved across ZAR1 orthologs (Figure 3A). Histidine (H) 488 and lysine (K) 195, located in the ADP/ATP binding pocket (Wang et al., 2019a; Wang et al., 2019b), are invariant in all 117 orthologs. In addition, three NB-ARC residues, W150, S152 and V154, known to form the NBD-NBD oligomerization interface for resistosome formation (Wang et al., 2019b; Hu et al., 2020), are present in 82-97% of the ZAR1 orthologs and were also part of a MEME motif (Figure 3A).

The N-terminal CC domain of Arabidopsis ZAR1 mediates cell death signalling thorough the N-terminal α1 helix/MADA motif, that becomes exposed in activated

ZAR1 resistosome to form a funnel like structure (Baudin et al., 2017; 2019; Wang et al., 2019b; Adachi et al., 2019b). We detected an N-terminal MEME motif that matches the α1 helix/MADA motif (Figure 3A). We also used the HMMER software (Eddy, 1998) to query the ZAR1 orthologs with a previously reported MADA motif-Hidden Markov Model (HMM) (Adachi et al., 2019b). This HMMER search detected a MADA-like sequence at the N-terminus of all 117 ZAR1 orthologs (Supplemental Data Set 1).

Taken together, based on the conserved motifs depicted in Figure 3A, we propose that angiosperm ZAR1 orthologs share the main functional features of Arabidopsis ZAR1: 1) effector recognition via RLCK binding, 2) remodelling of intramolecular interactions via ADP/ATP switch, 3) oligomerization via the NBD-NBD interface and 4) α1 helix/MADA motif-mediated activation of hypersensitive cell death.

ZAR1 resistosome displays conserved surfaces on RLCK binding sites and the inner glutamate ring

To identify additional conserved and variable features in ZAR1 orthologs, we used ConSurf (Ashkenazy et al., 2016) to calculate a conservation score for each amino acid and generate a diversity barcode for ZAR1 orthologs (Figure 3B). We then used the cryo-EM structures of Arabidopsis ZAR1 to determine how the ConSurf score map onto the 3D structures (Figure 3C, D and Figure 4). First, we found five major variable surfaces (VS1 to VS5) on the inactive ZAR1 monomer

structure (Figure 3C, D), as depicted in the ZAR1 diversity barcode (Figure 3B). VS1 comprises α2/α4 helices and a loop between α3 and α4 helices of the CC domain. VS2 and VS3 corresponds to α1/α2 helices of NBD and a loop between α2 and α3 helices of HD1, respectively. VS4 comprises a loop between WHD and LRR and first three helices of the LRR domain. VS5 is mainly derived from the last three helices of the LRR domain and the loops between these helices (Figure 3B, D).

Next, we examined highly conserved surfaces on inactive and active ZAR1 structures (Figure 4A, B). Consistent with the MEME analyses, we confirmed that highly conserved surfaces match to the RLCK binding interfaces (Figure 4A, B). We also confirmed that the N-terminal α1 helix/MADA motif is conserved on the resistosome surfaces, although the first four N- terminal amino acids are missing from the N terminus of the active ZAR1 cryo-EM structures (Figure 4B, C). We also noted sequence conservation at the glutamate rings (comprised of E11, E18, E130 and E134) inside the Arabidopsis ZAR1 resistosome (Supplemental Figure 5). Glutamic acid (E) 11 is conserved in 94% of ZAR1 orthologs, whereas only 3-18% retain E18, E130 and E134 in the same positions as Arabidopsis ZAR1. Interestingly, mutation of E11 to alanine (A) impaired Arabidopsis ZAR1-mediated cell death, but the E18A, E130A and E134A mutants were capable of inducing cell death (Bi et al., 2021). Furthermore, the E11A mutation impaired Ca^{2+} channel activity of the ZAR1 resistosome *in vitro* and *in vivo* (Bi et al., 2021). Therefore, our motif and structure analyses suggest that RLCK-mediated effector recognition and E11-dependent Ca^{2+} influx are key functional features conserved

across the great majority of ZAR1 orthologs.

ZAR1 interaction sites are conserved in ZED1-related kinase (ZRK) family proteins across distantly related plant species

We endeavored to experimentally test the hypothesis that ZAR1 ortholog proteins across angiosperm species require RLCKs to activate their molecular switch. First, we searched for RLCK XII-2 subfamily genes in the distantly related plant species, taro, stout camphor and columbine. The BLAST searches of protein databases were seeded with previously identified RLCK ZED1-related kinase (ZRK) sequences from Arabidopsis and *N. benthamiana* (Lewis et al., 2013; Schultink et al., 2019). We also performed iterated phylogenetic analyses using the kinase domain of the harvested ZRK-like sequences and obtained a well-supported clade that includes previously reported ZRK from Arabidopsis (ZRK1~7, 10~15) and *N. benthamiana* (JIM2) as well as new clade members from taro, stout camphor and columbine (Figure 5A). In total, we identified 21 ZRK genes in these species, which include one ZRK gene (CeZRK1) from taro, 15 ZRK genes (CmZRK1~15) from stout camphor and five ZRK genes (AcZRK1~5) from columbine (Figure 5A, Supplemental Data Set 4).

Remarkably, similar to Arabidopsis ZRKs (Lewis et al., 2013), a number of the identified ZRKs are located in genomic clusters. 13 ZRK genes in stout camphor and four ZRK genes in columbine form gene clusters on scaffold QPKB01000003.1 and contig KZ305039.1, respectively (Figure 5B). All of the

identified ZRK genes are located on a different scaffold or contig to the ZAR1 gene in taro, stout camphor and columbine, whereas Arabidopsis ZAR1 and the nine ZRK genes occur on the same chromosome (Supplemental Data Set 4).

The 21 ZRK genes code for proteins of 277-452 amino acids, similar to Arabidopsis and *N. benthamiana* ZRKs, which code for 269-396 amino acid proteins (Supplemental Data Set 5). ZRK family proteins from taro, stout camphor and columbine show 20.8 to 42.2% similarity to Arabidopsis RKS1/ZRK1 (Supplemental Data Set 6). Although the sequence similarity is low across the ZRK proteins in angiosperms, ZAR1 interaction sites are highly conserved in the ZRKs (Supplemental Figure 6) (Wang et al., 2019a; Hu et al., 2020). Notably, functionally validated residues for ZAR1-RLCK interactions [G27 and leucine 31 (L31) in Arabidopsis RKS1/ZRK1; G29 and asparatic acid (D) 231 in Arabidopsis ZED1/ZRK5] are conserved in 81 to 100% of the 21 ZRKs. Moreover, 90% of the 21 ZRKs have a hydrophobic V or I residue at the same position to V35 in Arabidopsis RKS1/ZRK1 (corresponding to I24 in Arabidopsis ZED1/ZRK5). This sequence conservation supports our hypothesis that ZRK family proteins function together with ZAR1 across distantly related plant species.

Heterologous expression of ZAR1 and ZRK orthologs from flowering plant species in *Nicotiana benthamiana*

To validate functional connections between ZAR1 orthologs and their partner ZRKs across angiosperm diversity, we cloned wild-type ZAR1 and ZRK genes

457 from taro, stout camphor and columbine. We also generated autoactive ZAR1
458 mutants by introducing a D to V mutation in the MHD motif following the approach
459 we previously used for NbZAR1 (NbZAR1^{D481V}; Harant et al., 2022). In a series of
460 experiments, we expressed the ZAR1 and ZRK genes separately or in
461 combination.
462
463 First, we examined whether wild-type and MHD mutants of ZAR1 are autoactive
464 in *N. benthamiana*. We expressed wild-type and MHD mutant of taro ZAR1
465 (CeZAR1^{WT}, CeZAR1^{D487V}), stout camphor ZAR1 (CmZAR1^{WT}, CmZAR1^{D488V})
466 and columbine ZAR1 (AcZAR1^{WT}, AcZAR1^{D489V}) to determine whether wild-type
467 and MHD mutant of these ZAR1 orthologs cause autoactive cell death in *N.*
468 *benthamiana*. The three orthologs behaved differently in these assays. Whereas
469 both AcZAR1^{WT} and AcZAR1^{D489V} induced autoactive cell death in *N.*
470 *benthamiana* leaves, only the D to V mutant of CeZAR1 (CeZAR1^{D487V}) elicited
471 cell death, and neither one of CmZAR1^{WT} and CmZAR1^{D488V} caused a cell death
472 response (Supplemental Figures 7). As controls, we expressed wild-type and D
473 to V mutant of Arabidopsis ZAR (AtZAR1^{WT}, AtZAR1^{D489V}) and *N. benthamiana*
474 ZAR1 (NbZAR1^{WT}, NbZAR1^{D481V}). As reported previously (Baudin et al., 2019;
475 Harant et al., 2022), NbZAR1^{D481V} triggered autoactive cell death in *N.*
476 *benthamiana* leaves, but AtZAR1^{D489V} did not (Supplemental Figures 7).
477
478 Next, to determine whether wild-type ZRKs from taro, stout camphor and
479 columbine trigger autoactive cell death in *N. benthamiana*, we screened 19 ZRKs
480 from taro (CeZRK1), stout camphor (CmZRK2, CmZRK3, CmZRK4, CmZRK5,

CmZRK6, CmZRK7, CmZRK8, CmZRK9, CmZRK10, CmZRK11, CmZRK12, CmZRK13, CmZRK15) and columbine (AcZRK1, AcZRK2, AcZRK3, AcZRK4, AcZRK5) (Pai et al., 2023). None of the tested ZRKs triggered macroscopic cell death response when expressed in *N. benthamiana* leaves (Supplemental Figure 8; Pai et al., 2023). These results indicate that taro, stout camphor and columbine ZRKs do not have autoactivity in *N. benthamiana*. This provides an opportunity to investigate functional connection between co-specific ZAR1 and ZRK orthologs by determining the effect of ZRK expression on ZAR1-mediated cell death response.

Stout camphor and columbine ZED1-related kinase (ZRK) proteins positively regulate the autoactive cell death of their co-specific ZAR1

To determine ZRK function in ZAR1-mediated cell death, we co-expressed D to V mutant of ZAR1 orthologs, CeZAR1^{D487V}, CmZAR1^{D488V} and AcZAR1^{D489V} with ZRK genes from each species. In these assays, CeZRK1 expression did not enhance cell death autoactivity of CeZAR1^{D487V}, whereas AcZRK1, AcZRK3, AcZRK4 and AcZRK5, but not AcZRK2, enhanced the cell death response of AcZAR1^{D489V} (Figure 6A, B; Supplemental Figure 8). Co-expression of CmZAR1^{D488V} together with CmZRK2, CmZRK6, CmZRK8, CmZRK9, CmZRK10, CmZRK11 or CmZRK13 caused macroscopic cell death in *N. benthamiana* leaves even though CmZAR1^{D488V} itself did not trigger visible cell death (Figure 6C, D).

We further conducted side-by-side experiments co-expressing of ZAR1 D to V mutants and ZRKs in comparison with single gene expression of either ZAR1 D to V mutants or ZRKs (Supplemental Figure 9). This confirmed that four columbine ZRKs (AcZRK1, AcZRK3, AcZRK4, AcZRK5) and seven stout camphor ZRKs (CmZRK2, CmZRK6, CmZRK8, CmZRK9, CmZRK10, CmZRK11, CmZRK13) positively regulate cell death activity of their co-specific ZAR1, although the ZRKs themselves did not show autoactivity in *N. benthamiana* (Supplemental Figure 9). These results indicate that the ZAR1 orthologs of these species are functionally associated with ZRKs as previously shown for Arabidopsis ZAR1 and *N. benthamiana* ZAR1. We conclude that ZAR1 has been partnering with RLCKs for over 150 Mya of angiosperm evolution.

Considering that the interaction surfaces between ZAR1 and ZRKs are well-conserved (Figure 4A), we hypothesized that ZAR1 and ZRK proteins may be functionally interchangeable between different plant species. To test this, we co-expressed Arabidopsis RKS1/ZRK1 with D to V mutant of Arabidopsis ZAR1 (AtZAR1), AcZAR1 and CmZAR1 in *N. benthamiana zar1-1* mutant line. As observed in original ZAR1-ZRK experiments (Figure 6), RKS1/ZRK1 positively regulated autoactive cell death by CmZAR1^{D488V} (Supplemental Figure 10). In the control experiment expressing AtZAR1^{D489V} and RKS1/ZRK1, RKS1/ZRK1 conferred autoactivity to AtZAR1 MHD mutant in the *N. benthamiana zar1-1* line (Supplemental Figure 10). These experiments further confirm that the immune function of ZAR1 and ZRK family proteins is conserved across different flowering plant species.

Our observation that the CeZAR1 autoactive mutant triggered cell death regardless of CeZRK1, raised the possibility that CeZAR1 functions together with the endogenous JIM2 RLCK in *N. benthamiana*. To test this, we used a hairpin-silencing construct of *JIM2* (RNAi:JIM2), that mediates silencing of *JIM2* when transiently expressed in *N. benthamiana* leaves (Harant et al., 2022). Silencing of endogenous *JIM2* did not affect the cell death activity of CeZAR1^{D487V}, although it suppressed cell death triggered by NbZAR1^{D481V} (Supplemental Figure 11). This result indicates that unlike *N. benthamiana* ZAR1, taro ZAR1 triggers autoactive cell death independently of JIM2.

Integration of a PLP3a thioredoxin-like domain at the C-termini of cassava and cotton ZAR1

As noted earlier, nine ZAR1 orthologs carry an integrated domain (ID) at their C-termini (Supplemental Data Set 1). These ZAR1-ID include two predicted proteins (XP_021604862.1 and XP_021604864.1) from *Manihot esculenta* (cassava) and seven predicted proteins (KAB1998109.1, PPD92094.1, KAB2051569.1, TYG89033.1, TYI49934.1, TYJ04029.1, KJB48375.1) from the cotton plant species *Gossypium barbadense*, *Gossypium darwinii*, *Gossypium mustelinum* and *Gossypium raimondii* (Supplemental Data Set 1). The integrations follow an intact LRR domain and the IDs vary in length from 108 to 266 amino acids (Figure 7A). We confirmed that the ZAR1-ID gene models of cassava XP_021604862.1 and XP_021604864.1 are correct based on RNA-seq

exon coverage in the NCBI database (database ID: LOC110609538). However, cassava ZAR1-ID XP_021604862.1 and XP_021604864.1 are isoforms encoded by transcripts from a single locus on chromosome LG2 (RefSeq sequence NC_035162.1) of the cassava RefSeq assembly (GCF_001659605.1) which also produces transcripts encoding isoforms lacking the C-terminal ID (XP_021604863.1, XP_021604865.1, XP_021604866.1, XP_021604867.1 and XP_021604868.1). Thus, cassava ZAR1-ID are probably splicing variants from a unique cassava ZAR1 gene locus.

To determine whether ZAR1-ID transcript is expressed in cassava, we analyzed public RNA-seq data from cassava samples in details (BioSample IDs in NCBI database: SAMN02950671, SAMN02950673, SAMN02950674, SAMN02950672 SAMN02444910, SAMN02444915, AMN02444919, SAMN05208186). We confirmed that RNA-seq reads detected from leaf and stem samples of 60444 and MCOL1522 cassava cultivars span between the end of LRR and beginning of Trx domain regions (Supplemental Figure 12). Notably, those reads are detected in the samples inoculated with the bacteria *Xanthomonas euvesicatoria* or *Xanthomonas axonopodis*, but not in their control samples (Supplemental Figure 12). Furthermore, three reads spanning LRR and Trx regions are detected in RNA-seq data from lateral bud of TME204 cultivar (Supplemental Figure 12). This suggests that ZAR1-ID is a splicing variant produced in cassava leaves and stems during *Xanthomonas* infection or in the specific tissue like lateral bud.

To determine the phylogenetic relationship between ZAR1-ID and canonical ZAR1, we mapped the domain architectures of ZAR1 orthologs on the phylogenetic tree shown in Figure 2 (Supplemental Figure 13). Cassava and cotton ZAR1-ID occur in different branches of the ZAR1 rosid clade indicating that they may have evolved as independent integrations although alternative evolutionary scenarios such as a common origin followed by subsequent deletion of the ID or lineage sorting remain possible (Supplemental Figure 13).

We annotated all the C-terminal extensions as thioredoxin-like using InterProScan (Trx, IPR036249; IPR013766; cd02989). The integrated Trx domain sequences are similar to Arabidopsis AT3G50960 (phosphoducin-like PLP3a; 34.8-90% similarity to integrated Trx domains), which is located immediately downstream of ZAR1 in a tail-to-tail configuration in the Arabidopsis genome (Supplemental Figure 14). We also noted additional genetic linkage between ZAR1 and Trx genes in other rosid species, namely field mustard, orange, cacao, grapevine and apple, and in the asterid species coffee (Supplemental Data Set 7). We conclude that ZAR1 is often genetically linked to a PLP3a-like Trx domain gene and that the integrated domain in ZAR1-ID has probably originated from a genetically linked sequence.

The ZAR1-SUB clade emerged early in eudicot evolution from a single ZAR1 duplication event

Phylogenetic analyses revealed ZAR1-SUB as a sister clade of the ZAR1

ortholog clade (Figure 1B, Figure 8). ZAR1-SUB clade comprises 129 genes from a total of 55 plant species (Supplemental Data Set 8). 21 of the 55 plant species carry a single-copy of ZAR1-SUB whereas 34 species have two or more copies (Supplemental Data Set 2). Of the 129 genes, 122 code for canonical CC-NLR proteins (692-1038 amino acid length) with shared sequence similarities ranging from 36.5 to 99.9% (Supplemental Data Set 8).

Unlike ZAR1, ZAR1-SUB NLRs are restricted to eudicots (Supplemental Figure 15, Supplemental Data Set 8). Three out of 129 genes are from the early diverging eudicot clade Ranunculales species, namely columbine, *Macleaya cordata* (plume poppy) and *Papaver somniferum* (opium poppy). The remaining ZAR1-SUB are spread across rosid and asterid species. We found that 11 species have ZAR1-SUB genes but lack a ZAR1 ortholog (Supplemental Data Set 2). These 11 species include two of the early diverging eudicots plume poppy and opium poppy, and the Brassicales *Carica papaya* (papaya). Interestingly, papaya is the only Brassicales species carrying a ZAR1-SUB gene, whereas the 16 other Brassicales species have ZAR1 but lack ZAR1-SUB genes (Supplemental Data Set 2). In total, we didn't detect ZAR1-SUB genes in 44 species that have ZAR1 orthologs, and these 44 species include the monocot taro, the magnoliid stout camphor and 42 eudicots, such as Arabidopsis, sugar beet and *N. benthamiana* (Supplemental Data Set 2).

In summary, given the taxonomic distribution of the ZAR1-SUB clade genes, we propose that ZAR1-SUB has emerged from a single duplication event of ZAR1

prior to the split between Ranunculales and other eudicot lineages about ~120-130 Mya based on the species divergence time estimate of Chaw et al. (2019).

ZAR1-SUB paralogs have significantly diverged from ZAR1

We investigated the sequence patterns of ZAR1-SUB proteins and compared them to the sequence features of canonical ZAR1 proteins that we identified earlier (Figure 3A). MEME analyses revealed several conserved sequence motifs (Supplemental Table 2). Especially, the MEME motifs in the ZAR1-SUB NB-ARC domain were similar to ZAR1 ortholog motifs (Supplemental Table 3). These include P-loop and MHD motifs, which are broadly conserved in NB-ARC of 97% and 100% of the ZAR1-SUB NLRs, respectively (Figure 9A). MEME also revealed sequence motifs in the ZAR1-SUB LRR domain that partially overlaps in position with the conserved ZAR1-RLCK interfaces (Figure 9A, Supplemental Figure 16). However, the ZAR1-SUB MEME motifs in the LRR domain were variable at the ZAR1-RLCK interface positions compared to ZAR1, and the motif sequences were markedly different between ZAR1-SUB and ZAR1 proteins (Figures 3A, 9A).

Remarkably, unlike ZAR1 orthologs, MEME did not predict conserved sequence pattern from a region corresponding to the MADA motif, indicating that these sequences have diverged across ZAR1-SUB proteins (Figure 9A). We confirmed the low frequency of MADA motifs in ZAR1-SUB proteins using HMMER

searches with only ~30% (38 out of 129) of the tested proteins having a MADA-like sequence (Supplemental Data Set 8, Figure 8). Moreover, conserved sequence patterns were not predicted for the NBD-NBD interface of the ZAR1 resistosome (Figure 9A, Supplemental Figure 16).

We generated a diversity barcode for ZAR1-SUB proteins using the ConSurf as we did earlier with ZAR1 orthologs (Figure 9B). This revealed that there are several conserved sequence blocks in each of the CC, NB-ARC and LRR domains, such as the regions corresponding to P-loop, MHD motif and the equivalent of the ZAR1-RLCK interfaces.

Next, we mapped the ConSurf conservation scores onto a homology model of a representative ZAR1-SUB protein (XP_004243429.1 from tomato) built based on the Arabidopsis ZAR1 cryo-EM structures (Supplemental Figure 17). As highlighted in Supplemental Figure 17B and C, conserved residues, such as MHD motif region in the WHD, are located inside of the monomer and resistosome structures. Interestingly, although the prior MEME prediction analyses revealed conserved motifs in positions matching the ZAR1-RLCK interfaces in the LRR domain, the ZAR1-SUB structure homology models displayed variable surfaces in this region (Supplemental Figure 17A). This indicates that the variable residues within these sequence motifs are predicted to be on the outer surfaces of the LRR domain and may reflect interaction with different ligands.

673 Taken together, these results suggest that unlike ZAR1 orthologs, the ZAR1-SUB
674 paralogs have divergent molecular patterns for regions known to be involved in
675 effector recognition, resistosome formation and activation of hypersensitive cell
676 death.
677
678 **Eleven tandemly duplicated ZAR1-CIN genes occur in a 500 kb cluster in**
679 **the *Cinnamomum micranthum* (stout camphor) genome**
680
681 The ZAR1-CIN clade, identified by phylogenetic analyses as a sister clade to
682 ZAR1 and ZAR1-SUB, consists of 11 genes from the magnoliid species stout
683 camphor (Figure 1B, Figure 8, Supplemental Data Set 9). 8 of the 11 ZAR1-CIN
684 genes code for canonical CC-NLR proteins with 63.8 to 98.9% sequence
685 similarities to each other, whereas the remaining 3 genes code for truncated NLR
686 proteins. Interestingly, all ZAR1-CIN genes occur in a ~500 kb cluster on scaffold
687 QPKB01000005.1 of the stout camphor genome assembly (GenBank assembly
688 accession GCA_003546025.1) (Supplemental Figure 18A, B). This scaffold also
689 contains the stout camphor ZAR1 ortholog (CmZAR1, RWR84015), which is
690 located 48 Mb from the ZAR1-CIN cluster (Supplemental Figure 18A, B). Based
691 on the observed phylogeny and gene clustering, we suggest that the ZAR1-CIN
692 cluster emerged from segmental duplication and expansion of the ancestral
693 ZAR1 gene after stout camphor split from the other examined ZAR1 containing
694 species.
695
696 We examined the expression of the eleven CmZAR1 and ZAR1-CIN genes in

seven tissues of *C. micranthum* based on the data of Chaw et al. (Chaw et al., 2019). The CmZAR1 gene is relatively highly expressed in seven different tissues of the stout camphor tree (Supplemental Figure 18C). In contrast, only five of the eleven ZAR1-CIN genes displayed detectable expression levels. Of these, two ZAR1-CIN genes (RWR85656 and RWR85657) had different expression patterns across the tissues. Whereas RWR85657 had the highest expression level in flowers, RWR85656 displayed the highest expression levels in stem and old leaf tissues (Supplemental Figure 18C). The implications of these observations remain unclear but may reflect different degrees of tissue specialization of the ZAR1-CIN genes.

Tandemly duplicated ZAR1-CIN display variable ligand binding interfaces on the LRR domain

We performed MEME and ConSurf analyses of the 8 intact ZAR1-CIN proteins as described above for ZAR1 and ZAR1-SUB. The ConSurf barcode revealed that although ZAR1-CIN proteins are overall conserved, their WHD region and LRR domain include some clearly variable blocks (Figure 9B). MEME analyses of ZAR1-CIN sequences revealed that like ZAR1 orthologs, the MADA, P-loop and MHD motifs match highly conserved blocks of the ZAR1-CIN ConSurf barcode (Figure 9B, C, Supplemental Tables 4 and 5). Consistently, 87.5% (7 out of 8) of the ZAR1-CIN proteins were predicted to have a MADA-type N-terminal sequence based on MADA-HMM analyses (Supplemental Data Set 9, Figure 8).

MEME picked up additional sequence motifs in ZAR1-CIN proteins that overlap in position with the NBD-NBD and ZAR1-RLCK interfaces (Figure 9C, Supplemental Figure 19). However, the sequence consensus at the NBD-NBD and ZAR1-RLCK interfaces indicated these motifs are more variable among ZAR1-CIN proteins relative to ZAR1 orthologs, and the motif sequences at both interfaces were markedly different from the matching region in ZAR1 (Figures 3A, 9C).

We also mapped the ConSurf conservation scores onto a homology model of a representative ZAR1-CIN protein (RWR85656.1) built based on the Arabidopsis ZAR1 cryo-EM structures (Supplemental Figure 17). This model revealed several conserved surfaces, such as on the α1 helix in the CC domain and the WHD of the NB-ARC domain (Supplemental Figure 17B, C). In contrast, the ZAR1-CIN structure homology models displayed highly varied surfaces especially in the LRR region matching the RLCK binding interfaces of ZAR1 (Supplemental Figure 17A). This sequence diversification on the LRR surface suggests that the ZAR1-CIN paralogs may have different host partner proteins and/or effector recognition specificities compared to ZAR1.

DISCUSSION

This study of ZAR1 macroevolution originated from phylogenomic analyses we initiated during the UK COVID-19 lockdown of March 2020. We performed iterated comparative sequence similarity searches of plant genomes using the

CC-NLR immune receptor ZAR1 as a query, and subsequent phylogenetic evaluation of the recovered ZAR1-like sequences. This revealed that ZAR1 is an ancient gene with 120 orthologs recovered from 88 species including monocot, magnoliid and eudicot plants. ZAR1 is an atypically conserved CC-NLR in these species with the gene phylogeny tracing species phylogeny, and consistent with the view that ZAR1 originated early in angiosperms during the Jurassic geologic period ~220 to 150 Mya (Figure 10A). This evolutionary model of ZAR1 is consistent with a recent study by Gong et al. (2022) that was published 1.5 years after we posted a preprint of the present paper (Adachi et al., 2020). The ortholog series enabled us to determine that resistosome sequences that are known to be functionally important and have remained highly conserved throughout the long evolutionary history of ZAR1. In addition, we experimentally validated the model that ZAR1 has been a partner with RLCKs for over 150 Mya through functional reconstruction of ZAR1-RLCK pairs from distantly related plant species (Figure 10B). The main unexpected feature among ZAR1 orthologs is the acquisition of a C-terminal thioredoxin-like domain in cassava and cotton species (Figure 7). Our phylogenetic analyses also indicated that ZAR1 duplicated twice throughout its evolution (Figure 10A). In the eudicots, ZAR1 spawned a large paralog family, ZAR1-SUB, which greatly diversified and often lost the typical sequence features of ZAR1. A second paralog, ZAR1-CIN, is restricted to a tandemly repeated 11-gene cluster in stout camphor. Overall, our findings map patterns of functional conservation, expansion and diversification onto the evolutionary history of ZAR1 and its paralogs.

ZAR1 most likely emerged prior to the split between monocots, Magnoliids and eudicots, which corresponds to ~220 to 150 Mya based on the dating analyses of Chaw et al. (2019). The origin of the angiosperms remains hotly debated with uncertainties surrounding some of the fossil record coupled with molecular clock analyses that would benefit from additional genome sequences of undersampled taxa (Coiro et al., 2019). Fu et al. (2018) and Cui et al. (2022) provided credence to an earlier emergence of angiosperms with the discovery of the fossil flowers *Nanjinganthus dendrostyla* and *Florigerminis jurassica*, respectively. These findings place the emergence of flowering plants at the Jurassic. It is tempting to speculate that ZAR1 emerged among these early flowering plants during the period when dinosaurs dominated planet earth.

NLRs are notorious for their rapid and dynamic evolutionary patterns even at the intraspecific level. In sharp contrast, ZAR1 is an atypical core NLR gene conserved in a wide range of angiosperm species (Figure 2). Nevertheless, Arabidopsis ZAR1 can recognize diverse bacterial pathogen effectors, including five different effector families distributed among nearly half of a collection of ~500 *Pseudomonas syringae* strains (Laflamme et al., 2020) and an effector AvrAC from *Xanthomonas campestris* (Wang et al., 2015). How did ZAR1 remain conserved throughout its evolutionary history while managing to detect a diversity of effectors? The answer to the riddle lies in the fact that ZAR1 effector recognition occurs via its partner RLCKs. ZRKs of the RLCK XII-2 subfamily rest in complex with inactive ZAR1 proteins and bait effectors by binding them directly or by recruiting other effector-binding RLCKs, such as the family VII PBS1-like

protein 2 (PBL2) (Lewis et al., 2013; Wang et al., 2015). These ZAR1-associated RLCKs are highly diversified not only in Arabidopsis (Lewis et al., 2013), but also in stout camphor and columbine, where RLCK XII-2 members occurring in expanded ZRK gene clusters (Figure 5). In the Arabidopsis ZRK cluster, RKS1/ZRK1 is required for recognition of *X. campestris* effector AvrAC (Wang et al., 2015) and ZRK3 and ZED1/ZRK5 are required for recognition of *P. syringae* effectors HopF2a and HopZ1a, respectively (Lewis et al., 2013; Seto et al., 2017). Therefore, as in the model discussed by Schultink et al. (2019) and Gong et al. (2022), ZRKs appear to have evolved as pathogen 'sensors' whereas ZAR1 acts as a conserved signal executor to activate immune response.

The MEME and ConSurf analyses are consistent with the model of ZAR1/RLCK evolution described above. ZAR1 is not just exceptionally conserved across angiosperms but it has also preserved sequence patterns that are key to resistosome-mediated immunity (Figures 3 and 4). Within the LRR domain, ZAR1 orthologs display highly conserved surfaces for RLCK binding (Figure 4). We conclude that ZAR1 has been guarding host kinases throughout its evolution ever since the Jurassic period. These findings strikingly contrast with observations recently made by Prigozhin and Krasileva (2020) on highly variable Arabidopsis NLRs (hvNLRs), which tend to have diverse LRR sequences. For instance, the CC-NLR RPP13 displays variable LRR surfaces across 62 Arabidopsis accessions, presumably because these regions are effector recognition interfaces that are caught in arms race coevolution with the oomycete pathogen *Hyaloperonospora arabidopsidis* (Prigozhin and Krasileva, 2020). The emerging

view is that the mode of pathogen detection (direct vs indirect recognition) drives an NLR evolutionary trajectory by accelerating sequence diversification at the effector binding site or by maintaining the binding interface with the partner guardee/decoy proteins (Prigozhin and Krasileva, 2020).

Our functional validation of ZAR1 and ZRKs from distantly related plant species supported the model that ZRKs function together with ZAR1 to trigger immune response *in planta* (Figure 6). 11 of the 19 tested ZRKs were either required or enhanced the autoactivity of their co-specific ZAR1 in *N. benthamiana*. The remaining eight tested ZRKs, CeZRK1, AcZRK2, CmZRK3, CmZRK4, CmZRK5, CmZRK7, CmZRK12 and CmZRK15 did not alter cell death activity of ZAR1. Notably, CmZRK4, CmZRK5 and CmZRK12 have N-terminal truncation or mutations at the ZAR1 interaction sites identified from the Arabidopsis ZAR1-ZRK studies (Supplemental Data Set 6). Therefore, some of the ZRK members may have lost their association with ZAR1 through deletion or mutations.

Taro and columbine ZAR1 could trigger autoactive cell death without their partner RLCKs in *N. benthamiana*, whereas stout camphor and *N. benthamiana* ZAR1 proteins require ZRKs to trigger the cell death response (Figure 6; Supplemental Figure 7) (Harant et al., 2022). In the case of taro and columbine, ZRKs may trigger conformational changes of ZAR1 after recognition of cognate pathogen effectors. In this scenario, autoactive ZAR1 could form a resistosome without ZRK proteins, thereby triggering the observed cell death response. In the future,

841 further comparative biochemical studies would further inform our understanding
842 of how ZAR1-ZRK interactions have evolved and contributed to ZAR1
843 resistosome formation across angiosperms.
844
845 ZAR1 orthologs display a patchy distribution across angiosperms (Supplemental
846 Data Set 1). Given the low number of non-eudicot species with ZAR1, it is
847 challenging to develop a conclusive evolutionary model. Nonetheless, the most
848 parsimonious explanation is that ZAR1 was lost in the monocot Commelinales
849 lineage (Figure 10A, Supplemental Data Set 1). ZAR1 is also missing in some
850 eudicot lineages, notably Fabales, Cucurbitales, Apiales and Asterales
851 (Supplemental Data Set 1). Cucurbitaceae (Cucurbitales) species are known to
852 have reduced repertoires of NLR genes possibly due to low levels of gene
853 duplications and frequent deletions (Lin et al., 2013). ZAR1 may have been lost in
854 this and other plant lineages as part of an overall shrinkage of their NLRomes or
855 as consequence of selection against autoimmune phenotypes triggered by NLR
856 mis-regulation (Karasov et al., 2017; Adachi et al., 2019a). Notably, plant linages
857 that don’t have a ZAR1 ortholog also lack ZRK family genes, suggesting that
858 ZAR1 and ZRK co-evolved to function in resistosome-mediated immunity across
859 angiosperms (Gong et al., 2022).
860
861 We unexpectedly discovered that some ZAR1 orthologs from cassava and
862 cotton species carry a C-terminal thioredoxin-like domain (ZAR1-ID in Figure 7).
863 Although Gong et al. (2022) suggested ZAR-IDs are annotation errors, we
864 confirmed that at least cassava ZAR1-Trx is expressed as a splicing variant in

leaf and stem inoculated with *Xanthomonas* bacteria or in lateral bud (Supplemental Figure 12). What is the function of these integrated domains? The occurrence of unconventional domains in NLRs is relatively frequent and ranges from 5 to 10% of all NLRs. In several cases, integrated domains have emerged from pathogen effector targets and became decoys that mediate detection of the effectors (Kourelis and van der Hoorn, 2018). Whether or not the integrated Trx domain of ZAR1-ID functions to bait effectors will need to be investigated. Since ZAR1-ID proteins still carry intact RLCK binding interfaces (Supplemental Data Set 10), they may have evolved dual or multiple recognition specificities via RLCKs and the Trx domain. In addition, all ZAR1-ID proteins have an intact N-terminal MADA motif (Supplemental Figure 13), suggesting that they probably can execute the hypersensitive cell death through their N-terminal CC domains even though they carry a C-terminal domain extension (Adachi et al., 2019b). In the future, it would be intriguing to understand how the ZAR1-ID splicing variant is produced and how the ZAR-ID function comparing to the ZAR1 resistosome model.

Our sequence analyses of ZAR1-ID indicate that the integrated Trx domain originates from the PLP3 phosphoducin gene, which is immediately downstream of ZAR1 in the Arabidopsis genome and adjacent to ZAR1 in several other eudicot species (Supplemental Figure 14). Whether or not PLP3 plays a role in ZAR1 function and the degree to which close genetic linkage facilitated domain fusion between these two genes are provocative questions for future studies.

ZAR1 spawned two classes of paralogs through two independent duplication events. The ZAR1-SUB paralog clade emerged early in the eudicot lineage—most likely tens of millions of years after the emergence of ZAR1—and has diversified into at least 129 genes in 55 species (Figure 10A). ZAR1-SUB proteins are distinctly more diverse in sequence than ZAR1 orthologs and generally lack key sequence features of ZAR1, like the MADA motif and the NBD-NBD oligomerization interface (Figure 9) (Adachi et al., 2019b; Wang et al., 2019b; Hu et al., 2020). This pattern is consistent with 'use-it-or-lose-it' evolutionary model, in which NLRs that specialize for pathogen detection lose some of the molecular features of their multifunctional ancestors (Adachi et al., 2019b). Therefore, we predict that many ZAR1-SUB proteins evolved into specialized sensor NLRs that require NLR helper mates for executing the hypersensitive response. It is possible that ZAR1-SUB helper mate is ZAR1 itself, and that these NLRs evolved into a phylogenetically linked network of sensors and helpers similar to the NRC network of asterid plants (Wu et al., 2017). However, 11 species have a ZAR1-SUB gene but lack a canonical ZAR1 (Supplemental Data Set 2), indicating that these ZAR1-SUB NLRs may have evolved to depend on other classes of NLR helpers.

How would ZAR1-SUB sense pathogens? Given that the LRR domains of most ZAR1-SUB proteins markedly diverged from the RLCK binding interfaces of ZAR1, it is unlikely that all of ZAR1-SUB members bind RLCKs in a ZAR1-type manner (Supplemental Figure 17). This leads us to draw the hypothesis that ZAR1-SUB proteins have diversified to recognize other ligands than RLCKs.

913 Indeed, Gong et al. (2022) showed that only *Populus trichocarpa* and *Prunus*
914 *persica* ZAR1-SUB (PtZAR1-SUB and PpZAR1-SUB) out of six tested
915 ZAR1-SUB members interacted with ZRK proteins in co-immunoprecipitation
916 experiments. Both PtZAR1-SUB and PpZAR1-SUB did not form ZAR1-like
917 oligomer complex with RKS1 and did not cause cell death response. Therefore,
918 ZAR1-SUB may require other components to be activated or execute immune
919 responses. In the future, functional investigations of ZAR1-SUB proteins could
920 provide insights into how multifunctional NLRs, such as ZAR1, evolve into
921 functionally specialized NLRs.
922
923 The ZAR1-CIN clade consists of 11 clustered paralogs that are unique to the
924 magnoliid species stout camphor as revealed from the genome sequence of the
925 Taiwanese small-flowered camphor tree (also known as *Cinnamomum kanehirae*,
926 Chinese name niu zhang 牛樟) (Chaw et al., 2019). This cluster probably
927 expanded from ZAR1, which is ~48 Mbp on the same genome sequence scaffold
928 (Supplemental Figure 18). The relatively rapid expansion pattern of ZAR1-CIN
929 into a tandemly duplicated gene cluster is more in line with the classical model of
930 NLR evolution compared to ZAR1 maintenance as a genetic singleton over tens
931 of millions of years (Michelmore and Meyers, 1998). ZAR1-CIN proteins may
932 have neofunctionalized after duplication, acquiring new recognition specificities
933 as consequence of coevolution with host partner proteins and/or pathogen
934 effectors. Consistent with this view, ZAR1-CIN exhibit different patterns of gene
935 expression across tissues (Supplemental Figure 18). Moreover, ZAR1-CIN
936 proteins display distinct surfaces at the ZAR1-RLCK binding interfaces and may

bind to other ligands than RLCKs as we hypothesized above for ZAR1-SUB (Supplemental Figure 16). ZAR1-CIN could be viewed as intraspecific highly variable NLRs (hvNLR) per the nomenclature of Prigozhin and Krasileva (2020).

Unlike ZAR1-SUB, ZAR1-CIN have retained the N-terminal MADA sequence (Figure 9, Supplemental Figure 17). We propose that ZAR1-CIN are able to execute the hypersensitive cell death on their own similar to ZAR1. However, ZAR1-CIN display divergent sequence patterns at NBD-NBD oligomerization interfaces compared to ZAR1 (Figure 9C, Supplemental Figure 19). Therefore, ZAR1-CIN may form resistosome-type complexes that are independent of ZAR1. One intriguing hypothesis is that ZAR1-CIN may associate with each other to form heterocomplexes of varying complexity and functionality operating as an NLR receptor network. In any case, the clear-cut evolutionary trajectory from ZAR1 to the ZAR1-CIN paralog cluster provides a robust evolutionary framework to study functional transitions and diversifications in this CC-NLR lineage.

In summary, our phylogenomics analyses raise several intriguing questions about ZAR1 evolution. The primary conclusion we draw is that ZAR1 is an ancient CC-NLR that has been a partner with RLCKs ever since the Jurassic Period. We propose that throughout at least 150 million years, ZAR1 has maintained its molecular features for sensing pathogens via RLCKs and activating hypersensitive cell death. Further comparative analyses, combining molecular evolution and structural biology, of plant resistosomes and between resistosomes and the apoptosomes and inflammasome of animal NLR systems (Wang and

Chai, 2020) will yield novel experimentally testable hypotheses for NLR research.

Materials and Methods

ZAR1 and ZRK sequence retrieval

We performed BLAST (Altschul et al., 1990) using previously identified ZAR1 and ZRK sequences as queries (Lewis et al., 2013; Baudin et al., 2017; Schultink et al., 2019; Harant et al., 2022) to search ZAR1 and ZRK like sequences in NCBI nr or nr/nt database (https://blast.ncbi.nlm.nih.gov/Blast.cgi) and Phytozome12.1 (https://phytozome.jgi.doe.gov/pz/portal.html#!search?show=BLAST). In the BLAST search, we used cut-offs, percent identity ≥ 30% and query coverage ≥ 80%. The BLAST pipeline was circulated by using the obtained sequences as new queries to search ZAR1 and ZRK like genes over the angiosperm species. We also performed the BLAST pipeline against a plant NLR dataset annotated by NLR-parser (Steuernagel et al., 2015) from 38 plant reference genome databases (Supplemental Data Set 11).

Phylogenetic analyses

For the phylogenetic analysis, we aligned NLR and ZRK amino acid sequences (Supplemental Data Sets 5, 12 to 16) using MAFFT v.7 (Katoh and Standley,

2013) and manually deleted the gaps in the alignments in MEGA7 (Kumar et al., 2016). Full-length or NB-ARC domain sequences of the aligned NLR datasets were used for generating phylogenetic trees. To generate ZRK phylogenetic trees, we used full-length or kinase domain sequences of the aligned ZRK datasets. The neighbor-joining tree was made using MEGA7 with JTT model and bootstrap values based on 100 iterations. All phylogenetic tree files are in Supplemental Data Sets 17 to 21.

Patristic distance analyses

To calculate the phylogenetic (patristic) distance, we used Python script based on DendroPy (Sukumaran and Mark, 2010). We calculated patristic distances from each CC-NLR to the other CC-NLRs on the phylogenetic tree and extracted the distance between CC-NLRs of Arabidopsis or *N. benthamiana* to the closest NLR from the other plant species. The script used for the patristic distance calculation is available from GitHub (https://github.com/slt666666/Phylogenetic_distance_plot2).

Gene co-linearity analyses

To investigate genetic co-linearity at ZAR1 loci, we extracted the 3 genes upstream and downstream of ZAR1 using GFF files derived from reference genome databases (Supplemental Data Set 11). To identify conserved gene blocks, we used gene annotation from NCBI Protein database and confirmed

protein domain information based on InterProScan (Jones et al, 2014).

Sequence conservation analyses

Full-length NLR sequences of each subfamily ZAR1, ZAR1-SUB or ZAR1-CIN were subjected to motif searches using the MEME (Multiple EM for Motif Elicitation) (Bailey and Elkan, 1994) with parameters 'zero or one occurrence per sequence, top twenty motifs', to detect consensus motifs conserved in ≥90% of the input sequences. The output data are summarized in Supplemental Tables 1, 2 and 4.

To predict the MADA motif from ZAR1, ZAR1-SUB and ZAR1-CIN datasets, we used the MADA-HMM previously developed (Adachi et al., 2019b), with the hmmsearch program (hmmsearch –max -o <outputfile> <hmmfile> <seqdb>) implemented in HMMER v2.3.2 (Eddy, 1998). We termed sequences over the HMMER cut-off score of 10.0 as the MADA motif and sequences having the score 0-to-10.0 as the MADA-like motif.

To analyze sequence conservation and variation in ZAR1, ZAR1-SUB and ZAR1-CIN proteins, aligned full-length NLR sequences (Supplemental Data Sets 10, 22, 23) were used for ConSurf (Ashkenazy et al., 2016). Arabidopsis ZAR1 (NP_190664.1), a tomato ZAR1-SUB (XP_004243429.1) or a Stout camphor ZAR1-CIN (RWR85656.1) was used as a query for each analysis of ZAR1, ZAR1-SUB or ZAR1-CIN, respectively. The output datasets are in Supplemental

Data Sets 24 to 26.

Protein structure analyses

The atomic coordinate of ZAR1 (protein data bank accession codes; 6J5T) was downloaded from protein data bank for illustration in ccp4mg. We used the cryo-EM structures of ZAR1 as templates to generate homology models of ZAR1-SUB and ZAR1-CIN. Amino acid sequences of a tomato ZAR1-SUB (XP_004243429.1) and a stout camphor ZAR1-CIN (RWR85656.1) were submitted to Protein Homology Recognition Engine V2.0 (Phyre2) for modelling (Kelley et a., 2015). The coordinates of ZAR1 structure (6J5T) were retrieved from the Protein Data Bank and assigned as modelling template by using Phyre2 Expert Mode. The resulting models of ZAR1-SUB and ZAR1-CIN, and the ZAR1 structures (6J5T) were illustrated with the ConSurf conservation scores in PyMol.

Plant growth condition

Wild-type *N. benthamiana* and *zar1-1* mutant plants (Schultink et al., 2019) were grown in a controlled growth chamber with temperature 22-25℃, humidity 45-65% and 16/8 hr light/dark cycle.

Plasmid constructions

The Golden Gate Modular Cloning (MoClo) kit (Weber et al., 2011) and the MoClo plant parts kit (Engler et al., 2014) were used for cloning, and all vectors are from this kit unless specified otherwise. ZAR1 and RLCK homologs identified in the taro (*Colocasia esculenta*; Assembly: ASM944546v1), columbine (*Aquilegia coerulea*; Assembly: Aquilegia_coerulea_v1; Filiault et al., 2018), and stout camphor tree (*Cinnamomum kanehirae*; Assembly: ASBRC_Ckan_1.0; Chaw et al., 2019) genomes were codon-optimized for *N. benthamiana* using the ThermoFisher GeneOptimizer tool and synthesized by GENEWIZ as Golden Gate Level 0 modules into pICH41155. Genes were subcloned into the binary vector pICH86988 (Weber et al., 2011) and transformed into *A. tumefaciens* strain GV3101 pMP90. Cloning design and sequence analysis were done using Geneious Prime (v2022.0.1; https://www.geneious.com). Plasmid construction is described in Supplemental Data Set 27.

Transient gene-expression and cell death assay

Transient expression of ZAR1 and RLCK homologs in *N. benthamiana* were performed by agroinfiltration according to methods described by Bos et al. (2006). Briefly, four-weeks old *N. benthamiana* plants were infiltrated with *Agrobacterium tumefaciens* strains carrying the binary expression plasmids. *A. tumefaciens* suspensions were prepared in infiltration buffer (10 mM MES, 10 mM $MgCl_2$, and 150 µM acetosyringone, pH5.6) and were adjusted to appropriate OD_{600} (Supplemental Data Set 27). Macroscopic cell death phenotypes were scored according to Supplemental Figure 20 and statistical

differences among the samples were analyzed with Tukey's HSD test (Supplemental Data Set 28).

RNA-seq data analyses

Public RNA-seq reads, which were previously obtained with Illumina HiSeq 2000 (Chaw et al., 2019), were used to analyze expression profiles of CmZAR1 and ZAR1-CIN genes in the stout camphor tree (Accession Numbers: SRR7416905, SRR7416906, SRR7416908, SRR7416909, SRR7416910, SRR7416911, and SRR7416918). Reads were mapped to the stout camphor genome assembly (GenBank assembly accession GCA_003546025.1) using the splice-aware RNAseq tool in CLC Genomics Workbench vs 20.0.4 (https://digitalinsights.qiagen.com) and transformed into a Transcripts Per Million (TPM) value according to Li et al. (2010). TPM values were visualized by the heatmap. The heatmap was colored by eight ranges (0, 0~5, 5~20, 20~40, 40~60, 60~80, 80~100, 100<) of TPM values.

RNA-seq reads (Accession Numbers: SRR1538828, SRR1538829, SRR1538848, SRR1538903, SRR1538904, SRR1538905, SRR1538928, SRR1538929, SRR1538930, SRR1538931, SRR1538932, SRR1538933, SRR1050891, SRR1050897, SRR1050892, SRR1050898, SRR3629840) were used to analyze MeZAR1-ID expression in cassava. RNA-seq reads were filtered and trimmed using fastp (Chen et al., 2018). The quality-trimmed reads were mapped to the cassava genome assembly (GenBank assembly accession

GCF_001659605.2) using HISAT2 (Kim et al., 2019). Mapped reads were analyzed using Integrative Genomics Viewer (Robinson et al., 2011).

Accession numbers

DNA sequence data used in this study can be found from reference genome or GenBank/EMBL databases with accession numbers listed in Supplemental Data Sets 1, 4, 8 and 9.

Supplemental Data

Supplemental Figure 1. Arabidopsis ZAR1 is the most conserved CC-NLR across angiosperms, supports Figure 1.

Supplemental Figure 2. NbZAR1 is highly conserved across angiosperms, supports Figure 1.

Supplemental Figure 3. Sequence alignment of full-length ZAR1 ortholog proteins across angiosperms, supports Figure 2.

Supplemental Figure 4. Schematic representation of the intragenomic relationship at ZAR1 loci across angiosperm genomes, supports Figure 2.

Supplemental Figure 5. E11 on glutamate ring inside of the Arabidopsis ZAR1 resistosome is conserved across the orthologs, supports Figure 4.

Supplemental Figure 6. Sequence alignment of full-length ZRK proteins across angiosperms, supports Figure 5.

Supplemental Figure 7. Heterologous expression of ZAR1 orthologs from

flowering plant species in *Nicotiana benthamiana*, supports Figure 6.

Supplemental Figure 8. *Colacasia esculenta* ZRK1 does not alter autoimmune cell death by *Colacasia esculenta* ZAR1 in *Nicotiana benthamiana*, supports Figure 6.

Supplemental Figure 9. Four *Aquilegia coerulea* ZRKs and seven *Cinnamomum micranthum* ZRKs positively regulate AcZAR1 and CmZAR1 autoactive cell death in *Nicotiana benthamiana*, supports Figure 6.

Supplemental Figure 10. Cell death assay by co-expressing Arabidopsis RKS1 with *Aquilegia coerulea* ZAR1 and *Cinnamomum micranthum* ZAR1 in *Nicotiana benthamiana*, supports Figure 6.

Supplemental Figure 11. Silencing of *JIM2* does not affect CeZAR1 autoactive cell death in *Nicotiana benthamiana*, supports Figure 6.

Supplemental Figure 12. Cassava ZAR1-ID is transcribed as a splicing variant from a single locus on the genome, supports Figure 7.

Supplemental Figure 13. Trx domain integration occurred in two independent rosid ZAR1 subclades, supports Figure 7.

Supplemental Figure 14. Integrated Trx domains show high sequence similarity to ZAR1-linked PLP3a gene in Arabidopsis, supports Figure 7.

Supplemental Figure 15. ZAR1-SUB gene is distributed across eudicots, supports Figure 8.

Supplemental Figure 16. Sequence alignment of full-length ZAR1 and ZAR1-SUB proteins, supports Figure 9.

Supplemental Figure 17. ZAR1 and the sister subclade NLRs display different conserved surfaces on the resistosome structure, supports Figure 9.

Supplemental Figure 18. ZAR1-CIN gene cluster occurs in the *Cinnamomum micranthum* genome, supports Figure 8.

Supplemental Figure 19. Sequence alignment of full-length ZAR1 and ZAR1-CIN proteins, supports Figure 9.

Supplemental Figure 20. Representative images for scoring cell death intensity as an HR index, supports Figure 6.

Supplemental Table 1. List of MEME motifs predicted from ZAR1 in angiosperms.

Supplemental Table 2. List of MEME motifs predicted from ZAR1-SUB.

Supplemental Table 3. Comparison of MEME motifs between ZAR1-SUB and ZAR1.

Supplemental Table 4. List of MEME motifs predicted from ZAR1-CIN.

Supplemental Table 5. Comparison of MEME motifs between ZAR1-CIN and ZAR1.

Supplemental Data Set 1. List of ZAR1 in angiosperms. 'NF' means 'not found'.

Supplemental Data Set 2. List of plant species with the number of ZAR1, ZAR1-SUB and ZAR1-CIN genes.

Supplemental Data Set 3. List of the closest NLR genes to ZAR1 locus.

Supplemental Data Set 4. Genome loci of ZAR1 and ZRK genes. 'NA' means 'not acquired'.

Supplemental Data Set 5. Amino acid sequences of full-length ZRKs.

Supplemental Data Set 6. Amino acid alignment file of 35 ZRK in angiosperms.

Supplemental Data Set 7. List of genes genetically linked to ZAR1 in eudicots. 'NF' means 'not found'.

Supplemental Data Set 8. List of ZAR1-SUB. ‘NF’ means ‘not found’.

Supplemental Data Set 9. List of ZAR1-CIN. ‘NF’ means ‘not found’.

Supplemental Data Set 10. Amino acid alignment file of 120 ZAR1 in angiosperms.

Supplemental Data Set 11. Reference genome databases used for NLR annotation with NLR-parser.

Supplemental Data Set 12. Amino acid sequences of full-length NLRs used for phylogenetic analysis in Figure 1B.

Supplemental Data Set 13. Amino acid sequences of full-length NLRs used for phylogenetic analysis in Supplemental Figure 1.

Supplemental Data Set 14. Amino acid sequences of 120 ZAR1 in angiosperms.

Supplemental Data Set 15. Amino acid sequences of 129 ZAR1-SUB.

Supplemental Data Set 16. Amino acid sequences of 11 ZAR1-CIN.

Supplemental Data Set 17. NLR phylogenetic tree file in Figure 1B.

Supplemental Data Set 18. NLR phylogenetic tree file in Supplemental Figure 1.

Supplemental Data Set 19. NLR phylogenetic tree file in Figure 2.

Supplemental Data Set 20. ZRK phylogenetic tree file in Figure 5A.

Supplemental Data Set 21. NLR phylogenetic tree file in Figure 8.

Supplemental Data Set 22. Amino acid alignment file of 129 ZAR1-SUB.

Supplemental Data Set 23. Amino acid alignment file of 11 ZAR1-CIN.

Supplemental Data Set 24. The ConSurf conservation score among ZAR1 proteins.

Supplemental Data Set 25. The ConSurf conservation score among ZAR1-SUB proteins.

Supplemental Data Set 26. The ConSurf conservation score among ZAR1-CIN proteins.

Supplemental Data Set 27. Plasmid list used in this study.

Supplemental Data Set 28. Summary of Tukey's HSD test results in cell death assay.

ACKNOWLEDGEMENTS

We are thankful to several colleagues for discussions and ideas. We thank Sebastian Schornack (Sainsbury Laboratory, University of Cambridge, Cambridge, UK) and Kodai Honda (Laboratory of Crop Evolution, Graduate School of Agriculture, Kyoto University) for valuable comments on this paper. This work was funded by the Gatsby Charitable Foundation, Biotechnology and Biological Sciences Research Council (BBSRC, UK), and European Research Council (ERC BLASTOFF projects). JLGH acknowledges support from the South Dakota Agricultural Experiment Station (SD00H605-16). H.A. was funded by the Japan Society for the Promotion of Science (21K20583 and 22K14893) and Japan Science and Technology Agency Precursory Research for Embryonic Science and Technology (JPMJPR21D1). We thank the Prime Minister of the United Kingdom for announcing a stay-at-home order on 23rd March 2020.

AUTHOR CONTRIBUTIONS

Conceptualization: H.A., S.K.; Data curation: H.A., T.S., J.K., H.P., J.L.G.H., A.M.; Formal analysis: H.A., T.S., A.M.; Investigation: H.A., T.S., A.M.; Methodology: H.A., T.S., J.K., A.M.; Resources: H.A., T.S., J.K., H.P., Y.U., M.S.; Supervision: H.A., A.M., S.K.; Funding acquisition: S.K.; Project administration: S.K.; Writing initial draft: H.A., J.K., S.K.; Editing: H.A., T.S., J.K., J.L.G.H., S.K.

DECLARATION OF INTERESTS

S.K. receives funding from industry on NLR biology.

References

Adachi H, Derevnina L, Kamoun S. (2019a) NLR singletons, pairs, and networks: evolution, assembly, and regulation of the intracellular immunoreceptor circuitry of plants. *Curr Opin Plant Biol* **50**:121-131. doi:10.1016/j.pbi.2019.04.007.

Adachi H, Contreras MP, Harant A, Wu CH, Derevnina L, Sakai T, Duggan C, Moratto E, Bozkurt TO, Maqbool A, Win J, Kamoun S. (2019b) An N-terminal motif in NLR immune receptors is functionally conserved across distantly related plant species. *eLife* **8:** e49956. doi: 10.7554/eLife.49956.

1249 Adachi H, Sakai T, Kourelis J, Maqbool A, Kamoun S. (2020) Jurassic NLR:
1250 conserved and dynamic evolutionary features of the atypically ancient
1251 immune receptor ZAR1. *bioRxiv* doi:
1252 https://doi.org/10.1101/2020.10.12.333484
1253 Altschul SF, Gish W, Miller W, Myers EW, Lipman DJ. (1990) Basic local
1254 alignment search tool. *J Mol Biol* **215**: 403-10. doi:
1255 10.1016/S0022-2836(05)80360-2.
1256 Ashkenazy H, Abadi S, Martz E, et al. (2016) ConSurf 2016: an improved
1257 methodology to estimate and visualize evolutionary conservation in
1258 macromolecules. *Nucleic Acids Res* **44**: W344-W350.
1259 doi:10.1093/nar/gkw408.
1260 Baggs E, Dagdas G, Krasileva KV. (2017) NLR diversity, helpers and integrated
1261 domains: making sense of the NLR IDentity. *Curr Opin Plant Biol* **38**: 59-67.
1262 doi:10.1016/j.pbi.2017.04.012.
1263 Bailey TL, Elkan C. (1994) Fitting a mixture model by expectation maximization
1264 to discover motifs in biopolymers. *Proc Int Conf Intell Syst Mol Biol* **2**:28-36.
1265 Baudin M, Hassan JA, Schreiber KJ, Lewis JD. (2017) Analysis of the ZAR1
1266 immune complex reveals determinants for immunity and molecular
1267 interactions. *Plant Physiol* **174**: 2038-2053. doi: 10.1104/pp.17.00441.
1268 Baudin M, Schreiber KJ, Martin EC, Petrescu AJ, Lewis JD. (2019)
1269 Structure-function analysis of ZAR1 immune receptor reveals key molecular
1270 interactions for activity. *Plant J* **101**: 352-370. doi: 10.1111/tpj.14547.
1271 Bayless AM, Nishimura MT. (2020) Enzymatic functions for Toll/Interleukin-1
1272 receptor domain proteins in the plant immune system. *Front Genet* **11**:539.

1273 doi:10.3389/fgene.2020.00539.
1274 Bentham AR, Zdrzalek R, De la Concepcion JC, Banfield MJ. (2018) Uncoiling
1275 CNLs: structure/Function approaches to understanding CC domain function in
1276 plant NLRs. *Plant and Cell Physiology* **59**:2398–2408. doi:
1277 https://doi.org/10.1093/pcp/pcy185.
1278 Benson DA, Cavanaugh M, Clark K, Karsch-Mizrachi I, Lipman DJ, Ostell J,
1279 Sayers EW. (2013) GenBank. *Nucleic Acids Res* **41**: D36-42. doi:
1280 10.1093/nar/gks1195.
1281 Bi G, Su M, Li N, et al. (2021) The ZAR1 resistosome is a calcium-permeable
1282 channel triggering plant immune signaling. *Cell* 184:3528-3541.e12. doi:
1283 10.1016/j.cell.2021.05.003.
1284 Bos JI, Kanneganti TD, Young C, Cakir C, Huitema E, Win J, Armstrong MR,
1285 Birch PR, Kamoun S. (2006) The C-terminal half of *Phytophthora infestans*
1286 RXLR effector AVR3a is sufficient to trigger R3a-mediated hypersensitivity
1287 and suppress INF1- induced cell death in *Nicotiana benthamiana*. *Plant J* **48**:
1288 165-176. doi: 10.1111/j.1365-313X.2006.02866.x.
1289 Boutrot F, Zipfel C. (2017) Function, discovery, and exploitation of plant pattern
1290 recognition receptors for broad-spectrum disease resistance. *Annu Rev*
1291 *Phytopathol* **55**: 257-286. doi:10.1146/annurev-phyto-080614-120106.
1292 Burdett H, Bentham AR, Williams SJ, et al. (2019) The plant "resistosome":
1293 structural insights into immune signaling. *Cell Host Microbe* **26**:193-201.
1294 doi:10.1016/j.chom.2019.07.020.
1295 Cesari S, Bernoux M, Moncuquet P, Kroj T, Dodds PN. (2014) A novel conserved
1296 mechanism for plant NLR protein pairs: the "integrated decoy" hypothesis.

Front Plant Sci **5**:606. doi:10.3389/fpls.2014.00606.

Chaw SM, Liu YC, Wu YW, et al. (2019) Stout camphor tree genome fills gaps in understanding of flowering plant genome evolution. *Nat Plants* **5**:63-73. doi:10.1038/s41477-018-0337-0.

Chen S, Zhou Y, Chen Y, Gu J. (2018) fastp: an ultra-fast all-in-one FASTQ preprocessor. *Bioinformatics* **34**: i884-i890. doi: 10.1093/bioinformatics/bty560.

Coiro M, Doyle JA, Hilton J. (2019) How deep is the conflict between molecular and fossil evidence on the age of angiosperms? *New Phytol* **223**: 83-99. doi: 10.1111/nph.15708.

Cui D-F, Hou Y, Yin P, Wang X. (2022) A Jurassic flower bud from China. *Geological Society, London* **521**:81-93. https://doi.org/10.1144/SP521-2021-122

Dangl JL, Horvath DM, Staskawicz BJ. (2013) Pivoting the plant immune system from dissection to deployment. *Science* **341**:746-751. doi:10.1126/science.1236011.

Delaux PM, Hetherington AJ, Coudert Y, et al. (2019) Reconstructing trait evolution in plant evo-devo studies. *Curr Biol* **29**:R1110-R1118. doi:10.1016/j.cub.2019.09.044.

Dodds PN, Rathjen JP. (2010) Plant immunity: towards an integrated view of plant-pathogen interactions. *Nat Rev Genet* **11**:539-548. doi:10.1038/nrg2812.

Duxbury Z, Wang S, MacKenzie CI, et al. (2020) Induced proximity of a TIR signaling domain on a plant-mammalian NLR chimera activates defense in

plants. *Proc Natl Acad Sci U S A* **117**: 18832-18839. doi:10.1073/pnas.2001185117.

Eddy SR. (1998) Profile hidden markov models. *Bioinformatics* **14**:755-763. DOI: https://doi.org/10.1093/ bioinformatics/14.9.755.

Engler C, Youles M, Gruetzner R, Ehnert TM, Werner S, Jones JD, Patron NJ, Marillonnet S. (2014) A golden gate modular cloning toolbox for plants. *ACS Synth Biol* **3**: 839-843. doi: 10.1021/sb4001504.

Feehan JM, Castel B, Bentham AR, Jones JD. (2020) Plant NLRs get by with a little help from their friends. *Curr Opin Plant Biol* **56**:99-108. doi:10.1016/j.pbi.2020.04.006.

Filiault DL, Ballerini ES, Mandáková T, et al. (2018) The *Aquilegia* genome provides insight into adaptive radiation and reveals an extraordinarily polymorphic chromosome with a unique history. *ELife* 7:e36426. doi: 10.7554/eLife.36426.

Fu Q, Diez JB, Pole M, et al. (2018) An unexpected noncarpellate epigynous flower from the Jurassic of China. *Elife* **7**: e38827. doi:10.7554/eLife.38827.

Gong Z, Qi J, Hu M, Bi G, Zhou JM, Han GZ. (2022) The origin and evolution of a plant resistosome. *Plant Cell* 34: 1600-1620. doi:10.1093/plcell/koac053.

Goodstein DM, Shu S, Howson R, Neupane R, Hayes RD, Fazo J, Mitros T, Dirks W, Hellsten U, Putnam N, Rokhsar DS. (2012) Phytozome: a comparative platform for green plant genomics. *Nucleic Acids Res* **40**: D1178-1186. doi: 10.1093/nar/gkr944.

Harant A, Pai H, Sakai T, Kamoun S, Adachi H. (2022) A vector system for fast-forward studies of the HOPZ-ACTIVATED RESISTANCE1 (ZAR1)

1345 resistosome in the model plant *Nicotiana benthamiana*. Plant Physiol. 188:
1346 70-80. doi: 10.1093/plphys/kiab471.
1347 Hu M, Qi J, Bi G, Zhou JM. (2020) Bacterial effectors induce oligomerization of
1348 immune receptor ZAR1 *in vivo*. *Mol Plant* pii: S1674-2052(20)30066-6. doi:
1349 10.1016/j.molp.2020.03.004.
1350 Jacob P, Kim NH, Wu F, et al. (2021) The plant immune receptors NRG1.1 and
1351 ADR1 are calcium influx channels. *bioRxiv* doi:
1352 https://doi.org/10.1101/2021.02.25.431980.
1353 Jones JD, Dangl JL. (2006) The plant immune system. *Nature* **444**: 323-329.
1354 doi:10.1038/nature05286.
1355 Jones JD, Vance RE, Dangl JL. (2016) Intracellular innate immune surveillance
1356 devices in plants and animals. *Science* **354**: aaf6395.
1357 doi:10.1126/science.aaf6395.
1358 Jones P, Binns D, Chang H, Fraser M, Li W, McAnulla C, McWilliam H, Maslen J,
1359 Mitchell A, Nuka G, Pesseat S, Quinn A, Sangrador-Vegas A, Scheremetjew
1360 M, Yong S, Lopez R, Hunter S. (2014) InterProScan 5: genome-scale protein
1361 function classification. *Bioinformatics* **30**: 1236-1240. doi:
1362 10.1093/bioinformatics/btu031.
1363 Jubic LM, Saile S, Furzer OJ, El Kasmi F, Dangl JL. (2019) Help wanted: helper
1364 NLRs and plant immune responses. *Curr Opin Plant Biol* **50**: 82-94.
1365 doi:10.1016/j.pbi.2019.03.013.
1366 Karasov TL, Chae E, Herman JJ, Bergelson J. (2017) Mechanisms to mitigate
1367 the trade-off between growth and defense. *Plant Cell* **29**: 666-680.
1368 doi:10.1105/tpc.16.00931.

1369 Katoh K, Standley DM. (2013) MAFFT multiple sequence alignment software
1370 version 7: improvements in performance and usability. *Mol Biol Evol* **30**:
1371 772-780. doi: 10.1093/molbev/mst010.
1372 Kelley LA, Mezulis S, Yates CM, Wass MN, Sternberg MJ. (2015) The Phyre2
1373 web portal for protein modeling, prediction and analysis. *Nat Protoc* **10**:
1374 845-858. doi: 10.1038/nprot.2015.053.
1375 Kourelis J, van der Hoorn RAL. (2018) Defended to the nines: 25 years of
1376 resistance gene cloning identifies nine mechanisms for R protein function.
1377 *The Plant Cell* **30**: 285-299. doi: https://doi.org/10.1105/tpc.17.00579.
1378 Kourelis J, Sakai T, Adachi H, Kamoun S. (2021) RefPlantNLR is a
1379 comprehensive collection of experimentally validated plant disease resistance
1380 proteins from the NLR family. *PLoS Biol* 19:e3001124. doi:
1381 10.1371/journal.pbio.3001124.
1382 Kroj T, Chanclud E, Michel-Romiti C, Grand X, Morel JB. (2016) Integration of
1383 decoy domains derived from protein targets of pathogen effectors into plant
1384 immune receptors is widespread. *New Phytol* **210**: 618-626.
1385 doi:10.1111/nph.13869.
1386 Kumar S, Stecher G, Tamura K. (2016) MEGA7: Molecular Evolutionary
1387 Genetics Analysis Version 7.0 for Bigger Datasets. *Mol Biol Evol* **33**:
1388 1870-1874. doi: 10.1093/molbev/msw054.
1389 Laflamme B, Dillon MM, Martel A, Almeida RND, Desveaux D, Guttman DS.
1390 (2020) The pan-genome effector-triggered immunity landscape of a
1391 host-pathogen interaction. *Science* **367**: 763-768.
1392 doi:10.1126/science.aax4079.

1393 Lee H-Y, Mang H, Choi E-H, Seo Y-E, Kim M-S, Oh S, Kim S-B, Choi D. (2020)
1394 Genome-wide functional analysis of hot pepper immune receptors reveals an
1395 autonomous NLR cluster in seed plants. *bioRxiv* doi:
1396 https://doi.org/10.1101/2019.12.16.878959.
1397 Lee RRQ, Chae E. (2020) Variation patterns of NLR clusters in *Arabidopsis*
1398 *thaliana* genomes. *Plant Communications*
1399 https://doi.org/10.1016/j.xplc.2020.100089.
1400 Lewis JD, Wu R, Guttman DS, Desveaux D. (2010) Allele-specific virulence
1401 attenuation of the *Pseudomonas syringae* HopZ1a type III effector via the
1402 *Arabidopsis* ZAR1 resistance protein. *PLoS Genet* **6:** e1000894. doi:
1403 10.1371/journal.pgen.1000894.
1404 Lewis JD, Lee AH, Hassan JA, et al. (2013) The *Arabidopsis* ZED1
1405 pseudokinase is required for ZAR1-mediated immunity induced by the
1406 *Pseudomonas syringae* type III effector HopZ1a. *Proc Natl Acad Sci U S A*.
1407 **110**: 18722-18727. doi:10.1073/pnas.1315520110.
1408 Li, Bo, Ruotti, Victor, Stewart, Ron M., Thomson, James A., Dewey, Colin N.
1409 (2010) RNA-Seq gene expression estimation with read mapping uncertainty.
1410 *Bioinformatics* **26**: 493-500. doi:10.1093/bioinformatics/btp692.
1411 Liang X, Zhou JM. (2018) Receptor-like cytoplasmic kinases: central players in
1412 plant receptor kinase-mediated signaling. *Annu Rev Plant Biol* **69**: 267-299.
1413 doi:10.1146/annurev-arplant-042817-040540.
1414 Lin X, Zhang Y, Kuang H, Chen J. (2013) Frequent loss of lineages and deficient
1415 duplications accounted for low copy number of disease resistance genes in
1416 Cucurbitaceae. *BMC Genomics* **14**: 335. doi:10.1186/1471-2164-14-335.

1417 Ma S, Lapin D, Liu L, et al. (2020) Direct pathogen-induced assembly of an NLR
1418 immune receptor complex to form a holoenzyme. *Science* **370**: eabe3069.
1419 doi: 10.1126/science.abe3069.
1420 Martin R, Qi T, Zhang H, Liu F, King M, Toth C, Nogales E, Staskawicz BJ.
1421 (2020) Structure of the activated ROQ1 resistosome directly recognizing the
1422 pathogen effector XopQ. *Science* **370**: eabd9993. doi:
1423 10.1126/science.abd9993.
1424 Mermigka G, Amprazi M, Mentzelopoulou A, Amartolou A, Sarris PF. (2020)
1425 Plant and animal innate immunity complexes: fighting different enemies with
1426 similar weapons. *Trends Plant Sci* **25**: 80-91.
1427 doi:10.1016/j.tplants.2019.09.008.
1428 Michelmore RW, Meyers BC. (1998) Clusters of resistance genes in plants
1429 evolve by divergent selection and a birth-and-death process. *Genome Res* **8**:
1430 1113-1130. doi:10.1101/gr.8.11.1113.
1431 Pai H, Kourelis J, Adachi H, Kamoun S (2023) ZED1-related kinases (ZRKs)
1432 from *Aquilegia coerulea* and *Cinnamomum micranthum* do not trigger
1433 autoactive cell death in *Nicotiana benthamiana*. Zenodo
1434 https://doi.org/10.5281/zenodo.7844723.
1435 Prigozhin DM, Krasileva KV. (2020) Intraspecies diversity reveals a subset of
1436 highly variable plant immune receptors and predicts their binding sites.
1437 *bioRxiv* doi: https://doi.org/10.1101/2020.07.10.190785.
1438 Robinson JT, Thorvaldsdóttir H, Winckler W, Guttman M, Lander ES, Getz G,
1439 Mesirov JP. (2011) Integrative genomics viewer. *Nat Biotechnol* **29**: 24-26.
1440 doi: 10.1038/nbt.1754.

1441 Sarris PF, Cevik V, Dagdas G, Jones JD, Krasileva KV. (2016) Comparative
1442 analysis of plant immune receptor architectures uncovers host proteins likely
1443 targeted by pathogens. *BMC Biol* **14**: 8. doi:10.1186/s12915-016-0228-7.
1444 Seong K, Seo E, Witek K, Li M, Staskawicz B. (2020) Evolution of NLR
1445 resistance genes with noncanonical N-terminal domains in wild tomato
1446 species. *New Phytol* **227**: 1530-1543. doi:10.1111/nph.16628.
1447 Seto D, Koulena N, Lo T, Menna A, Guttman DS, Desveaux D. (2017) Expanded
1448 type III effector recognition by the ZAR1 NLR protein using ZED1-related
1449 kinases. *Nat Plants* **3**: 17027. doi:10.1038/nplants.2017.27.
1450 Schultink A, Qi T, Bally J, Staskawicz B. (2019) Using forward genetics in
1451 *Nicotiana benthamiana* to uncover the immune signaling pathway mediating
1452 recognition of the *Xanthomonas perforans* Effector XopJ4. *New Phytol* **221**:
1453 1001-1009. doi: 10.1111/nph.15411.
1454 Smith SA, Brown JW. (2018) Constructing a broadly inclusive seed plant
1455 phylogeny. *Am J Bot* **105**: 302-314. doi:10.1002/ajb2.1019.
1456 Shao ZQ, Xue JY, Wu P, et al. (2016) Large-scale analyses of angiosperm
1457 nucleotide-binding site-leucine-rich repeat genes reveal three anciently
1458 diverged classes with distinct evolutionary patterns. *Plant Physiol* **170**:
1459 2095-2109. doi:10.1104/pp.15.01487.
1460 Stam R, Silva-Arias GA, Tellier A. (2019) Subsets of NLR genes show differential
1461 signatures of adaptation during colonization of new habitats. *New Phytol* **224**:
1462 367-379. doi:10.1111/nph.16017.
1463 Steuernagel B, Jupe F, Witek K, Jones JD, Wulff BB. (2015) NLR-parser: rapid
1464 annotation of plant NLR complements. *Bioinformatics* **31**: 1665-1667. doi:

10.1093/bioinformatics/btv005.

Sukumaran J, Holder MT. (2010) DendroPy: a Python library for phylogenetic computing. *Bioinformatics* **26**: 1569-1571. doi: 10.1093/bioinformatics/btq228.

Tamborski J, Krasileva KV. (2020) Evolution of plant NLRs: from natural history to precise modifications. *Annu Rev Plant Biol* **71**: 355-378. doi:10.1146/annurev-arplant-081519-035901.

Uehling J, Deveau A, Paoletti M. (2017) Do fungi have an innate immune response? An NLR-based comparison to plant and animal immune systems. *PLoS Pathog* **13**: e1006578. doi:10.1371/journal.ppat.1006578.

Van de Weyer AL, Monteiro F, Furzer OJ, et al. (2019) A species-wide inventory of NLR genes and alleles in *Arabidopsis thaliana*. *Cell* **178**: 1260-1272.e14. doi:10.1016/j.cell.2019.07.038.

Wang G, Roux B, Feng F, et al. (2015) The decoy substrate of a pathogen effector and a pseudokinase specify pathogen-induced modified-self recognition and immunity in plants. *Cell Host Microbe* **18**: 285-295. doi:10.1016/j.chom.2015.08.004.

Wang J, Wang J, Hu M, W Shan, Qi J, Wang G, Han Z, Qi Y, Gao N, Wang H-W, Zhou J-M, Chai J. (2019a) Ligand-triggered allosteric ADP release primes a plant NLR complex. *Science* **364**: eaav5868. doi: 10.1126/science.aav5868.

Wang J, Hu M, Wang J, Qi J, Han Z, Wang G, Qi Y, Wang H-W, Zhou J-M, Chai J. (2019b) Reconstitution and structure of a plant NLR resistosome conferring immunity. *Science* **364**: eaav5870. doi: 10.1126/science.aav5870.

Wang J, Chai J. (2020) Structural Insights into the Plant Immune Receptors PRRs and NLRs. *Plant Physiol* **182**: 1566-1581. doi:10.1104/pp.19.01252.

Weber E, Engler C, Gruetzner R, Werner S, Marillonnet S. (2011) A modular cloning system for standardized assembly of multigene constructs. *PLoS One* **6**: e16765. doi: 10.1371/journal.pone.0016765.

Wu CH, Krasileva KV, Banfield MJ, Terauchi R, Kamoun S. (2015) The "sensor domains" of plant NLR proteins: more than decoys? *Front Plant Sci* **6**: 134. doi:10.3389/fpls.2015.00134.

Wu CH, Abd-El-Haliem A, Bozkurt TO, et al. (2017) NLR network mediates immunity to diverse plant pathogens. *Proc Natl Acad Sci U S A* **114**: 8113-8118. doi:10.1073/pnas.1702041114.

Wu CH, Derevnina L, Kamoun S. (2018) Receptor networks underpin plant immunity. *Science* **360**: 1300-1301. doi:10.1126/science.aat2623.

Xiong Y, Han Z, Chai J. (2020) Resistosome and inflammasome: platforms mediating innate immunity. *Curr Opin Plant Biol* **56**: 47-55. doi:10.1016/j.pbi.2020.03.010.

Zhou JM, Zhang Y. (2020) Plant immunity: danger perception and signaling. *Cell* **181**: 978-989. doi:10.1016/j.cell.2020.04.028.

Figure legends

Figure 1. Comparative sequence analyses identify and classify ZAR1 sequences from angiosperms. (**A**) Workflow for computational analyses in searching ZAR1 orthologs. We performed TBLASTN/BLASTP searches and subsequent phylogenetic analyses to identify ZAR1 ortholog genes from plant genome/proteome datasets. (**B**) ZAR1 forms a clade with two closely related sister subclades. The phylogenetic tree was generated in MEGA7 by the neighbor-joining method using NB-ARC domain sequences of ZAR1-like proteins identified from the prior BLAST searches and 1019 NLRs identified from 6 representative plant species, taro, stout camphor, columbine, tomato, sugar beet and Arabidopsis. Each branch is marked with different colors based on the ZAR1 and the sister subclades. Red arrow heads indicate bootstrap support > 0.7 and is shown for the relevant nodes. The scale bar indicates the evolutionary distance in amino acid substitution per site.

Figure 2. ZAR1 gene is distributed across angiosperms. The phylogenetic tree was generated in MEGA7 by the neighbor-joining method using full length amino acid sequences of 120 ZAR1 orthologs identified in Figure 1. Each branch is marked with different colors based on the plant taxonomy. Red triangles indicate bootstrap support > 0.7. The scale bar indicates the evolutionary distance in amino acid substitution per site.

Figure 3. ZAR1 orthologs carry conserved sequence patterns required for

Arabidopsis ZAR1 resistosome function. (**A**) Schematic representation of the Arabidopsis ZAR1 protein highlighting the position of conserved sequence patterns across ZAR1 orthologs. Consensus sequence patterns were identified by MEME using 117 ZAR1 ortholog sequences. Raw MEME motifs are listed in Supplemental Table 1. Red asterisks indicate residues functionally validated in Arabidopsis ZAR1 for NBD-NBD and ZAR1-RLCK interfaces. (**B**) Conservation and variation of each amino acid among ZAR1 orthologs across angiosperms. Amino acid alignment of 117 ZAR1 orthologs was used for conservation score calculation via the ConSurf server (https://consurf.tau.ac.il). The conservation scores are mapped onto each amino acid position in Arabidopsis ZAR1 (NP_190664.1). (**C, D**) Distribution of the ConSurf conservation score on the Arabidopsis ZAR1 structure. The inactive ZAR1 monomer is illustrated in cartoon representation with different colors based on each canonical domain (C) and the conservation score (D). Major five variable surfaces (VS1 to VS5) on the inactive ZAR1 monomer structure are described in grey dot or black boxes in panel B or D, respectively.

Figure 4. ZAR1 orthologs across angiosperms display multiple conserved surfaces on the resistosome structure. Distribution of the ConSurf conservation score was visualized on the inactive monomer (**A**), active monomer (**B**) and resistosome (**C**) structures of Arabidopsis ZAR1. Each structure and cartoon representation are illustrated with different colors based on the conservation score shown in Figure 3.

Figure 5. ZRK gene clusters occur in *Aquilegia coerulea* and *Cinnamomum micranthum*. (**A**) The phylogenetic tree was generated in MEGA7 by the neighbor-joining method using full length amino acid sequences of 39 ZRK proteins. Each branch is marked with different colors based on the plant taxonomy. Red triangles indicate bootstrap support > 0.7. The scale bar indicates the evolutionary distance in amino acid substitution per site. (**B**) Schematic representation of the ZRK gene clusters on an *A. coerulea* (columbine) contig and a *C. micranthum* (Stout camphor) scaffold.

Figure 6. ZRK family proteins positively regulate *Aquilegia coerulea* AcZAR1 and *Cinnamomum micranthum* CmZAR1 autoimmune cell death in *Nicotiana benthamiana*. (**A, C**) Cell death observed in *N. benthamiana* after expression of ZAR1 mutants with or without wild-type ZRKs. *N. benthamiana* leaf panels expressing wild-type NbZAR1 ($NbZAR1^{WT}$), $NbZAR1^{D481V}$ ($ZAR1^{D481V}$), $AcZAR1^{D489V}$ ($AcZAR1^{DV}$) and $CmZAR1^{D488V}$ ($CmZAR1^{DV}$) with or without wild-type ZRKs, were photographed at four days after agroinfiltration. (**B, D**) Violin plots show AcZAR1 and CmZAR1 cell death intensity scored as an HR index based on 12 and nine replicates (different leaves from independent plants) in two independent experiments. Different colors of plots describe data from different experiments. Statistical differences among the samples were analyzed with Tukey's HSD test ($p<0.01$).

Figure 7. Cassava and cotton ZAR1-ID carry an additional Trx domain at the C terminus. (**A**) Schematic representation of NLR domain architecture with

C-terminal Trx domain. (**B**) Description of Trx domain sequences on amino acid sequence alignment. Cassava XP_021604862.1 (MeZAR1) and cotton KAB1998109.1 (GbZAR1) were used for MAFFT version 7 alignment as representative ZAR1-ID. Arabidopsis ZAR1 (AtZAR1) was used as a control of ZAR1 without ID.

Figure 8. ZAR1-SUB has emerged early in eudicots and diverged at MADA motif sequence. The phylogenetic tree was generated in MEGA7 by the neighbor-joining method using full length amino acid sequences of 120 ZAR1, 129 ZAR1-SUB and 11 ZAR1-CIN identified in Figure 1. Each branch is marked with different colors based on the plant taxonomy. Red triangles indicate bootstrap support > 0.7. The scale bar indicates the evolutionary distance in amino acid substitution per site. NLR domain architectures are illustrated outside of the leaf labels: MADA is red, CC is pink, NB-ARC is yellow, LRR is blue and other domain is orange. Black asterisks on domain schemes describe truncated NLRs or potentially mis-annotated NLR.

Figure 9. Conserved sequence distributions in ZAR1-SUB and ZAR1-CIN. (**A**) Schematic representation of the ZAR1-SUB protein highlighting the position of the representative conserved sequence patterns across ZAR1-SUB. Representative consensus sequence patterns identified by MEME are described on the scheme. Raw MEME motifs are listed in Supplemental Tables 2 and 3. (**B**) Conservation and variation of each amino acid among ZAR1-SUB and ZAR1-CIN. Amino acid alignment of 129 ZAR1-SUB or 8 ZAR1-CIN was used

for conservation score calculation via the ConSurf server (https://consurf.tau.ac.il). The conservation scores are mapped onto each amino acid position in queries XP_004243429.1 (ZAR1-SUB) and RWR85656.1 (ZAR1-CIN), respectively. (**C**) Schematic representation of the ZAR1-CIN protein highlighting the position of the representative conserved sequence patterns across 8 ZAR1-CIN. Raw MEME motifs are listed in Supplemental Tables 4 and 5.

Figure 10. Co-evolution of ZAR1 and ZRK genes in angiosperms. (**A**) We propose that the ancestral ZAR1 gene has emerged ~220 to 150 million years ago (Mya) before monocot and eudicot lineages split. ZAR1 gene is widely conserved CC-NLR in angiosperms, but it is likely that ZAR1 has lost in a monocot lineage, Commelinales. A sister clade paralog ZAR1-SUB has emerged early in the eudicot lineages and may have lost in Caryophyllales. Another sister clade paralog ZAR1-CIN has duplicated from ZAR1 gene and expanded in the Magnoliidae *C. micranthum*. Trx domain integration to C terminus of ZAR1 has independently occurred in few rosid lineages. (**B**) ZAR1 has co-evolved with partner ZRK gene for pathogen effector recognition since the Jurassic era. During the co-evolution, ZRKs were diversified to catch up with fast-evolving effectors.

Supplemental Figure 1. Arabidopsis ZAR1 is the most conserved CC-NLR across angiosperms, supports Figure 1. (**A**) Phylogenetic tree of NLR proteins from 8 plant species. The phylogenetic tree was generated in MEGA7

by the neighbor-joining method using NB-ARC domain sequences of 1475 NLRs identified from taro, stout camphor, columbine, Arabidopsis, cassava, sugar beet, tomato and *N. benthamiana*. The scale bars indicate the evolutionary distance in amino acid substitution per site. We used CC-NLR and CC_{G10}-NLR superclades for calculating phylogenetic distances. (**B**) The phylogenetic (patristic) distance of two CC-NLR nodes between Arabidopsis and other plant species were calculated from the phylogeny shown in panel A, as previously described in Harant et al. (2022). Color of plots describe plant species.

Supplemental Figure 2. NbZAR1 is highly conserved across angiosperms, supports Figure 1. The phylogenetic (patristic) distance of two CC-NLR nodes between *N. benthamiana* and the closest NLR from the other plant species were calculated from the phylogeny in Supplemental Figure 1, as previously described in Harant et al. (2022).

Supplemental Figure 3. Sequence alignment of full-length ZAR1 ortholog proteins across angiosperms, supports Figure 2. Amino acid sequences of ZAR1 orthologs were aligned by MAFFT version 7 program. Conserved motif sequences highlighted in this study are marked with red boxes. Red asterisks indicate substitution sites for introducing gain or loss of ZAR1 protein function.

Supplemental Figure 4. Schematic representation of the intragenomic relationship at ZAR1 loci across angiosperm genomes, supports Figure 2. We selected representative 8 plant species genome assemblies based on the

phylogenetic tree in Figure 2 and used them for the synteny-based analysis of the ZAR1 loci. We highlight genes showing intragenomic linkages with different colors based on the gene annotations. Genes genetically linked to ZAR1 in eudicots are listed in Supplemental Data Set 7.

Supplemental Figure 5. E11 on glutamate ring inside of the Arabidopsis ZAR1 resistosome is conserved across the orthologs, supports Figure 4. The ConSurf conservation scores at E11 and E18 (**A**) or at E130 and E134 (**B**) are illustrated in cartoon representation of the Arabidopsis ZAR1 resistosome structure.

Supplemental Figure 6. Sequence alignment of full-length ZRK proteins across angiosperms, supports Figure 5. Amino acid sequences of ZRK proteins were aligned by MAFFT version 7 program. Functionally validated residues for ZRK-ZAR1 interactions are marked with red boxes.

Supplemental Figure 7. Heterologous expression of ZAR1 orthologs from flowering plant species in *Nicotiana benthamiana*, supports Figure 6. (**A**) Macroscopic cell death observed in *N. benthamiana* leaves after expression of wild-type and MHD mutant of ZAR1 orthologs. *N. benthamiana* leaves expressing wild-type *Nicotiana benthamiana* ZAR1 ($NbZAR1^{WT}$), $NbZAR1^{D481V}$ ($NbZAR1^{DV}$), wild-type *Arabidopsis thaliana* ZAR1 ($AtZAR1^{WT}$), $AtZAR1^{D489V}$ ($AtZAR1^{DV}$), wild-type *Colacasia esculenta* CeZAR1 ($CeZAR1^{WT}$), $CeZAR1^{D487V}$ ($CeZAR1^{DV}$), wild-type *Cinnamomum micranthum* ZAR1 ($CmZAR1^{WT}$),

CmZAR1^{D488V} (CmZAR1^{DV}), wild-type *Aquilegia coerulea* ZAR1 (AcZAR1^{WT}) and AcZAR1^{D489V} (AcZAR1^{DV}), were photographed at five days after agroinfiltration. Images are representative from 26 replicates (different leaves from independent plants) in three independent experiments. (**B**) Summary table of cell death response caused by wild-type and MHD mutant of ZAR1 orthologs in *N. benthamiana* leaves. Symbols "+" and "-" describe macroscopic cell death induction and no macroscopic cell response, respectively.

Supplemental Figure 8. *Colacasia esculenta* ZRK1 does not alter autoimmune cell death by *Colacasia esculenta* ZAR1 in *Nicotiana benthamiana*, supports Figure 6. (A) *N. benthamiana* leaf panels expressing wild-type NbZAR1 (NbZAR1^{WT}), NbZAR1^{D481V} (ZAR1^{D481V}), wild-type *Colacasia esculenta* CeZAR1 (CeZAR1^{WT}), CeZAR1^{D487V} (CeZAR1^{DV}) with empty vector control (EV) or without wild-type *Colacasia esculenta* ZRK1 (CeZRK1), were photographed at six days after agroinfiltration. (**B**) Violin plots show cell death intensity scored as an HR index based on 14 replicates (different leaves from independent plants) in two independent experiments. Different colors of plots describe data from different experiments. Statistical differences among the samples were analyzed with Tukey's HSD test ($p<0.01$). (C) Summary table of cell death response caused by co-expression of CeZAR1 and CeZRK1 in *N. benthamiana* leaves. Symbols "+" and "-" describe macroscopic cell death induction and no macroscopic cell response, respectively. "NT" indicates "not tested".

Supplemental Figure 9. Four *Aquilegia coerulea* ZRKs and seven *Cinnamomum micranthum* ZRKs positively regulate AcZAR1 and CmZAR1 autoactive cell death in *Nicotiana benthamiana*, supports Figure 6. Macroscopic cell death observed in *N. benthamiana* after co-expression of ZAR1 mutants and wild-type ZRKs, compared to single gene expression of ZAR1 mutants or wild-type ZRKs. (**A, B**) AcZAR1^{D489V} (AcZAR1^{DV}), wild-type AcZRKs and empty vector control (EV) were co-expressed in *N. benthamiana* leaves. (**C – E**) CmZAR1^{D488V} (CmZAR1^{DV}), wild-type CmZRKs and EV were co-expressed in *N. benthamiana* leaves. Photographs were taken at five days after agroinfiltration. Violin plots show AcZAR1 and CmZAR1 cell death intensity scored as an HR index based on 122 to 26 replicates (different leaves from independent plants) in three independent experiments. Different colors of plots describe data from different experiments. Statistical differences among the samples were analyzed with Tukey's HSD test ($p<0.01$).

Supplemental Figure 10. Cell death assay by co-expressing Arabidopsis RKS1 with *Aquilegia coerulea* ZAR1 and *Cinnamomum micranthum* ZAR1 in *Nicotiana benthamiana*, supports Figure 6. Cell death observed in *N. benthamiana zar1-1* mutant line after expression of wild-type and MHD mutant of ZAR1 with or without wild-type RKS1. *N. benthamiana* leaf panels expressing wild-type *Arabidopsis thaliana* ZAR1 (AtZAR1^{WT}), AtZAR1^{D489V} (AtZAR1^{DV}), wild-type *Nicotiana benthamiana* ZAR1 (NbZAR1^{WT}), NbZAR1^{D481V} (NbZAR1^{DV}), wild-type *Aquilegia coerulea* ZAR1 (AcZAR1^{WT}), AcZAR1^{D489V} (AcZAR1^{DV}), wild-type *Cinnamomum micranthum* ZAR1 (CmZAR1^{WT}) and CmZAR1^{D488V}

(CmZAR1^{DV}) with empty vector control (EV) or wild-type *Arabidopsis thaliana* RKS1 (RKS1), were photographed at four days after agroinfiltration. Images of macroscopic cell death response are representative from 10 and 11 replicates (different leaves from independent plants) in two independent experiments. Images of AtZAR1 and NbZAR1 cell death control are representative from 8 replicates (different leaves from independent plants). (**B**) Summary table of cell death response caused by co-expressing wild-type and MHD mutant of ZAR1 orthologs with RKS1 in *N. benthamiana* leaves. Symbols "+" and "-" describe macroscopic cell death induction and no macroscopic cell response, respectively.

Supplemental Figure 11. Silencing of *JIM2* does not affect CeZAR1 autoactive cell death in *Nicotiana benthamiana*, supports Figure 6. (**A**) Cell death observed in *N. benthamiana* leaves after expression of autoactive NbZAR1 (NbZAR1^{DV}) and CeZAR1 (CeZAR1^{DV}) with RNAi constructs. *N. benthamiana* leaf panels were photographed at six days after agroinfiltration. (**B**) Violin plots show cell death intensity scored as an HR index based on 18 replicates (different leaves from independent plants) in two independent experiments. Different colors of plots describe data from different experiments. Statistical differences among the samples were analyzed with Tukey's HSD test ($p<0.01$).

Supplemental Figure 12. Cassava ZAR1-ID is transcribed as a splicing variant from a single locus on the genome, supports Figure 7. (A) RNA-seq

reads span between LRR and Trx integrated domain (ID) regions of cassava ZAR1 (MeZAR1). Cassava sample information and BioSample IDs of the public RNA-seq data are listed. (**B**) Description of amino acid sequences on the boundary of LRR and Trx domains. 'NA' means 'not acquired'.

Supplemental Figure 13. Trx domain integration occurred in two independent rosid ZAR1 subclades, supports Figure 7. The phylogenetic tree shown in Figure 2 was used to describe NLR domain architectures. Domain schemes are aligned to right side of the leaf labels: MADA is red, CC is pink, NB-ARC is yellow, LRR is blue and other domain is orange. Black asterisks on domain schemes describe truncated NLRs or potentially mis-annotated NLR. Each branch is marked with different colors based on the plant taxonomy. Red triangles indicate bootstrap support > 0.7. The scale bar indicates the evolutionary distance in amino acid substitution per site.

Supplemental Figure 14. Integrated Trx domains show high sequence similarity to ZAR1-linked PLP3a gene in Arabidopsis, supports Figure 7. (**A**) Schematic representation of the intragenomic relationship at ZAR1 loci between Arabidopsis and cassava. We highlight sequence similarity of integrated Trx domain in Cassava ZAR1 (MeZAR1) to PLP3a gene genetically linked to Arabidopsis ZAR1 (AtZAR1). Details are explained in Supplemental Figure 4. (**B**) Amino acid sequences of Arabidopsis PLP3a gene (AT3G50960) and integrated domains of an MeZAR1 (XP_021604862.1) and a cotton ZAR1 (GbZAR1; KAB1998109.1).

Supplemental Figure 15. ZAR1-SUB gene is distributed across eudicots, supports Figure 8. The phylogenetic tree was generated in MEGA7 by the neighbor-joining method using full length amino acid sequences of 129 ZAR1-SUB orthologs identified in Figure 1. Each branch is marked with different colors based on the plant taxonomy. Red triangles indicate bootstrap support > 0.7. The scale bar indicates the evolutionary distance in amino acid substitution per site. Red asterisks on plant order term describe that NLRs from Malpighiales are distributed in three independent clades.

Supplemental Figure 16. Sequence alignment of full-length ZAR1 and ZAR1-SUB proteins, supports Figure 9. (**A**) Schematic representation of the ZAR1-SUB protein highlighting the position of the representative conserved sequence patterns across ZAR1-SUB. (**B**) Amino acid sequences of ZAR1 orthologs and a representative ZAR1-SUB (XP_004243429.1 from tomato) were aligned by MAFFT version 7 program. ZAR1 motif sequences highlighted in this study are marked with red boxes. Positions of MEME motifs identified from ZAR1-SUB are marked in blue boxes. Raw MEME motifs are listed in Supplemental Tables 2 and 3.

Supplemental Figure 17. ZAR1 and the sister subclade NLRs display different conserved surfaces on the resistosome structure, supports Figure 9. Distribution of the ConSurf conservation score was visualized on the inactive monomer (**A**), active monomer (**B**) and resistosome structures (**C-E**) of

Arabidopsis ZAR1 or the structure homology models of ZAR1-SUB (XP_004243429.1) and ZAR1-CIN (RWR85656.1). Each structure and cartoon representation are illustrated with different colors based on the conservation score shown in Figures 3 and 9. Resistosome structures are shown from different angles, from side (C), from upper side (D) and from underside (E).

Supplemental Figure 18. ZAR1-CIN gene cluster occurs in the *Cinnamomum micranthum* genome, supports Figure 8. (**A**) The subclades including ZAR1, ZAR1-SUB and ZAR1-CIN were zoomed in from the phylogenetic tree constructed in Supplemental Figure 1. Red triangles indicate bootstrap support > 0.7. The scale bar indicates the evolutionary distance in amino acid substitution per site. Well supported subclades (I and II) in ZAR1-CIN are described with red or blue dot box. The gene IDs: taro (MQM-), stout camphor (RWR-), columbine (Aqcoe-), Arabidopsis (AT-), cassava (Manes-), sugar beet (Bv-), tomato (Solyc-) and *N. benthamiana* (NbS-). (**B**) Schematic representation of the ZAR1-CIN gene cluster on a *C. micranthum* (Stout camphor) scaffold. Stout camphor ZAR1 (CmZAR1) and ZAR1-CIN genes are highlighted in orange and yellow, respectively. (**C**) A heatmap showing Transcripts Per Million (TPM) values of the CmZAR1 and ZAR1-CIN genes. Public RNA-seq datasets from seven different tissue samples in *C. micranthum* were used for this heatmap analysis.

Supplemental Figure 19. Sequence alignment of full-length ZAR1 and ZAR1-CIN proteins, supports Figure 9. (**A**) Schematic representation of the

ZAR1-CIN protein highlighting the position of the representative conserved sequence patterns across ZAR1-SUB. (**B**) Amino acid sequences of ZAR1 orthologs and a representative ZAR1-CIN (RWR85656.1) were aligned by MAFFT version 7 program. ZAR1 motif sequences highlighted in this study are marked with red boxes. Positions of MEME motifs identified from ZAR1-CIN are marked in orange boxes. Raw MEME motifs are listed in Supplemental Tables 4 and 5.

Supplemental Figure 20. Representative images for scoring cell death intensity as an HR index, supports Figure 6.

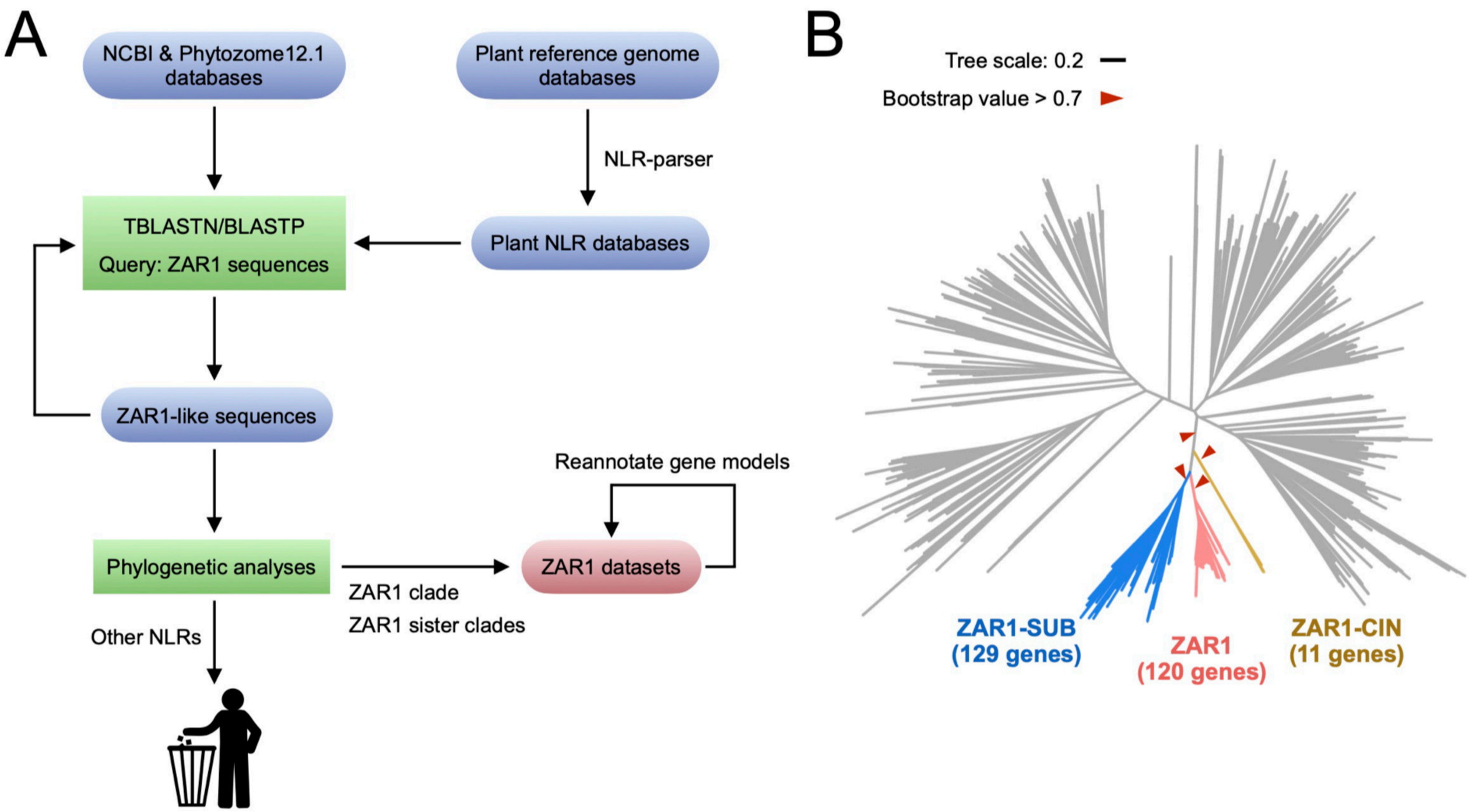

Figure 1. Comparative sequence analyses identify and classify ZAR1 sequences from angiosperms. (**A**) Workflow for computational analyses in searching ZAR1 orthologs. We performed TBLASTN/BLASTP searches and subsequent phylogenetic analyses to identify ZAR1 ortholog genes from plant genome/proteome datasets. (**B**) ZAR1 forms a clade with two closely related sister subclades. The phylogenetic tree was generated in MEGA7 by the neighbor-joining method using NB-ARC domain sequences of ZAR1-like proteins identified from the prior BLAST searches and 1019 NLRs identified from 6 representative plant species, taro, stout camphor, columbine, tomato, sugar beet and Arabidopsis. Each branch is marked with different colors based on the ZAR1 and the sister subclades. Red arrow heads indicate bootstrap support > 0.7 and is shown for the relevant nodes. The scale bar indicates the evolutionary distance in amino acid substitution per site.

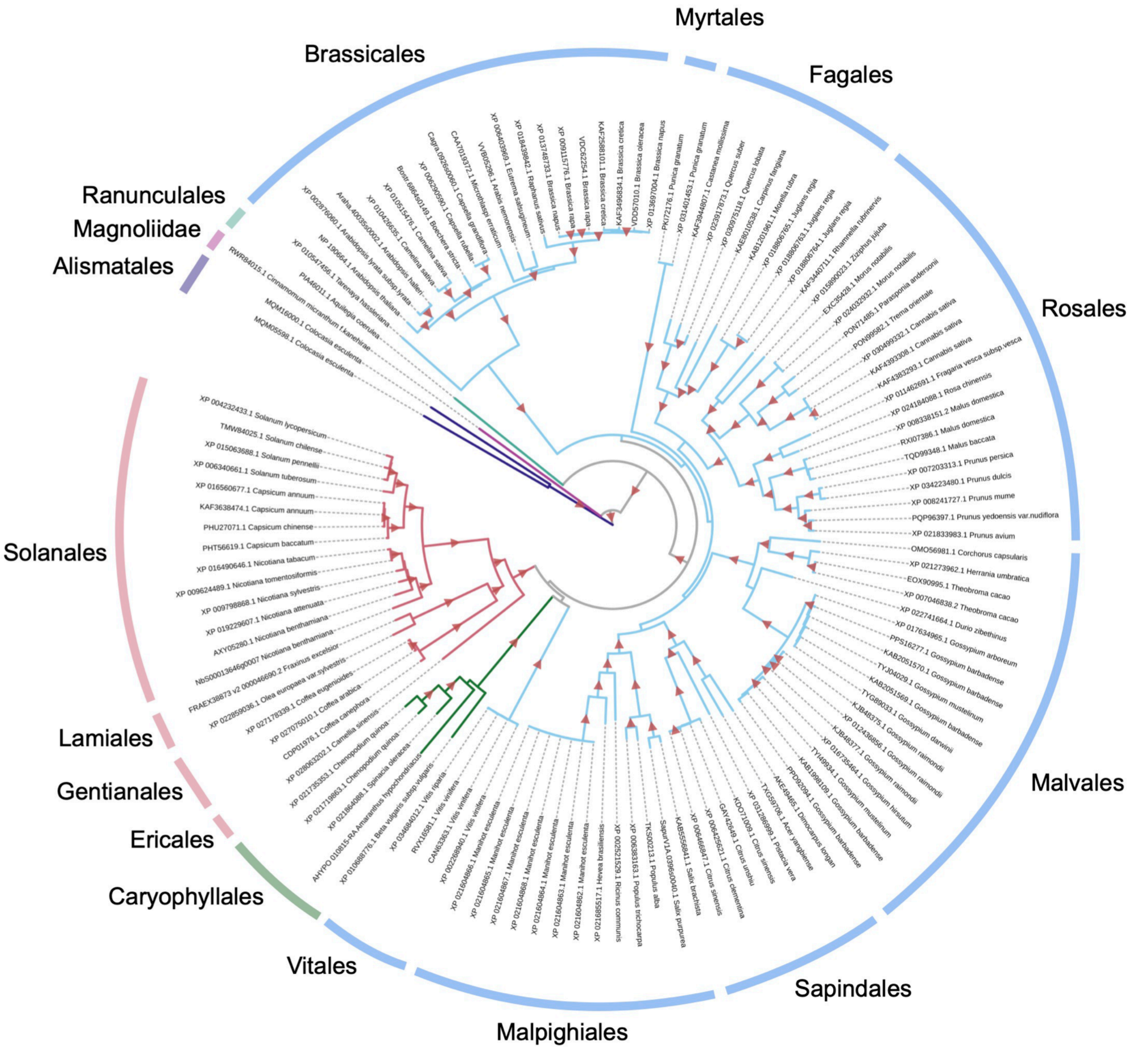

Figure 2. ZAR1 gene is distributed across angiosperms. The phylogenetic tree was generated in MEGA7 by the neighbor-joining method using full length amino acid sequences of 120 ZAR1 orthologs identified in Figure 1. Each branch is marked with different colors based on the plant taxonomy. Red triangles indicate bootstrap support > 0.7. The scale bar indicates the evolutionary distance in amino acid substitution per site.

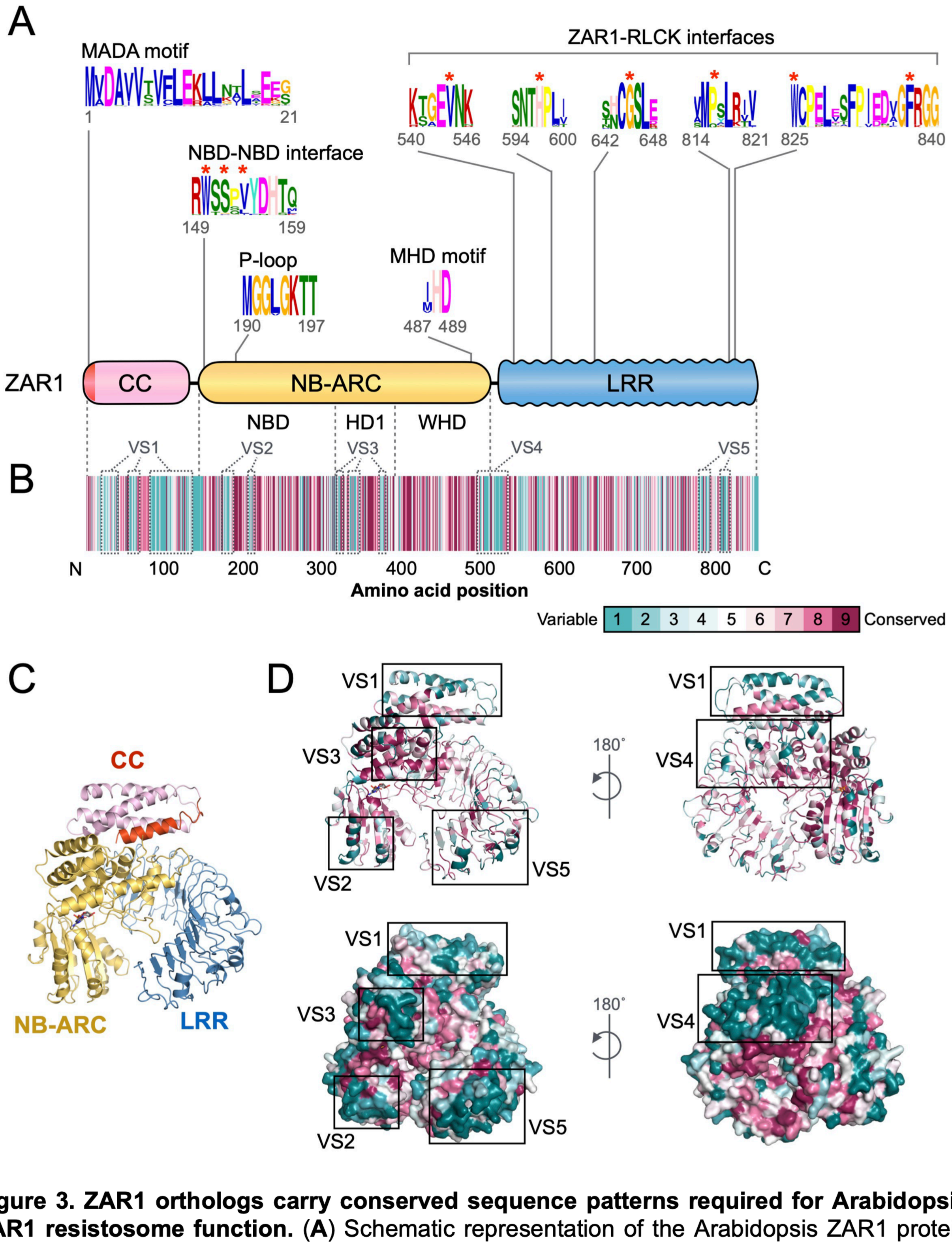

Figure 3. ZAR1 orthologs carry conserved sequence patterns required for Arabidopsis ZAR1 resistosome function. (**A**) Schematic representation of the Arabidopsis ZAR1 protein highlighting the position of conserved sequence patterns across ZAR1 orthologs. Consensus sequence patterns were identified by MEME using 117 ZAR1 ortholog sequences. Raw MEME motifs are listed in Supplemental Table 1. Red asterisks indicate residues functionally validated in Arabidopsis ZAR1 for NBD-NBD and ZAR1-RLCK interfaces. (**B**) Conservation and variation of each amino acid among ZAR1 orthologs across angiosperms. Amino acid alignment of 117 ZAR1 orthologs was used for conservation score calculation via the ConSurf server (https://consurf.tau.ac.il). The conservation scores are mapped onto each amino acid position in Arabidopsis ZAR1 (NP_190664.1). (**C, D**) Distribution of the ConSurf conservation score on the Arabidopsis ZAR1 structure. The inactive ZAR1 monomer is illustrated in cartoon representation with different colors based on each canonical domain (C) and the conservation score (D). Major five variable surfaces (VS1 to VS5) on the inactive ZAR1 monomer structure are described in grey dot or black boxes in panel B or D, respectively.

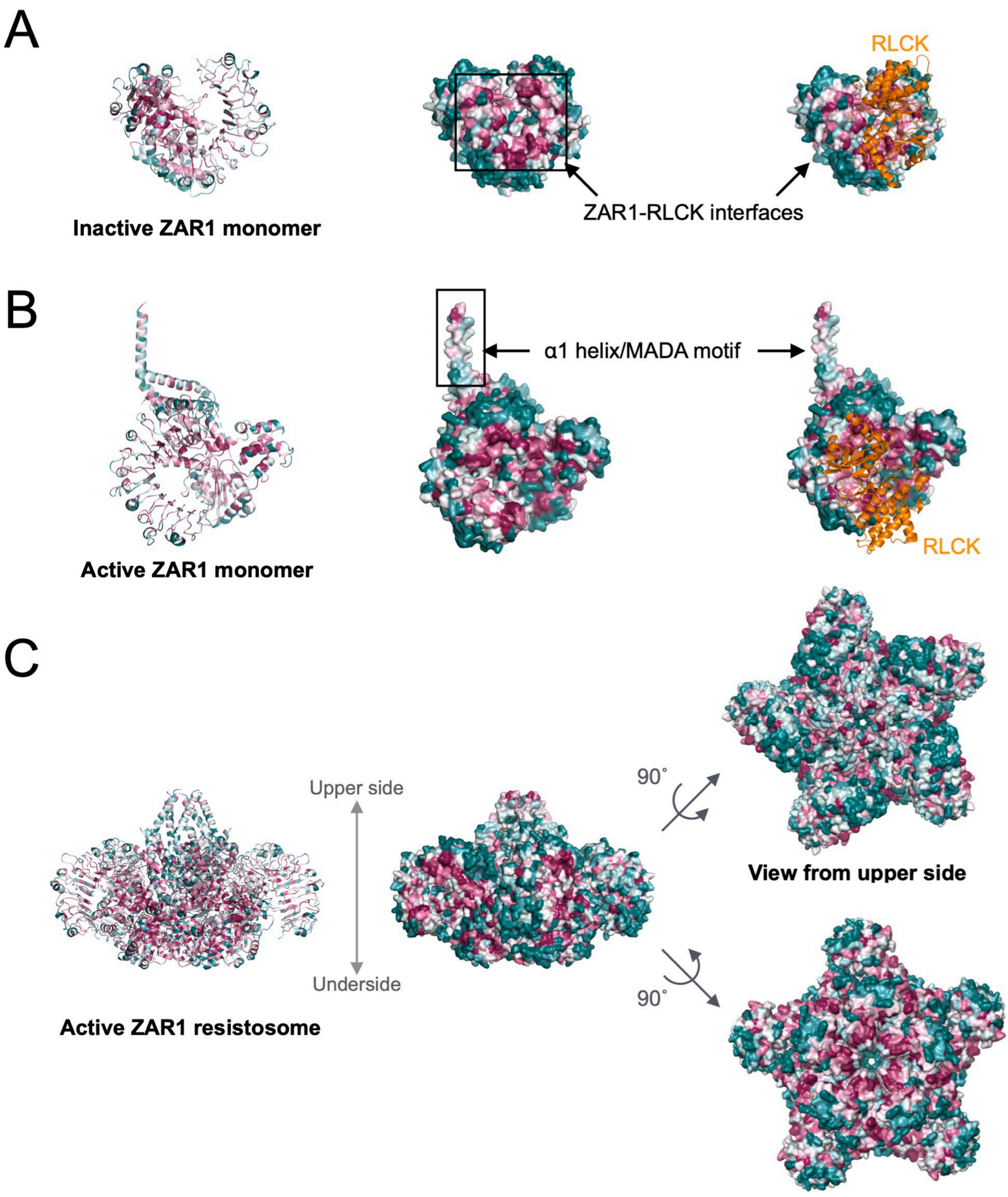

Figure 4. ZAR1 orthologs across angiosperms display multiple conserved surfaces on the resistosome structure. Distribution of the ConSurf conservation score was visualized on the inactive monomer (**A**), active monomer (**B**) and resistosome (**C**) structures of Arabidopsis ZAR1. Each structure and cartoon representation are illustrated with different colors based on the conservation score shown in Figure 3.

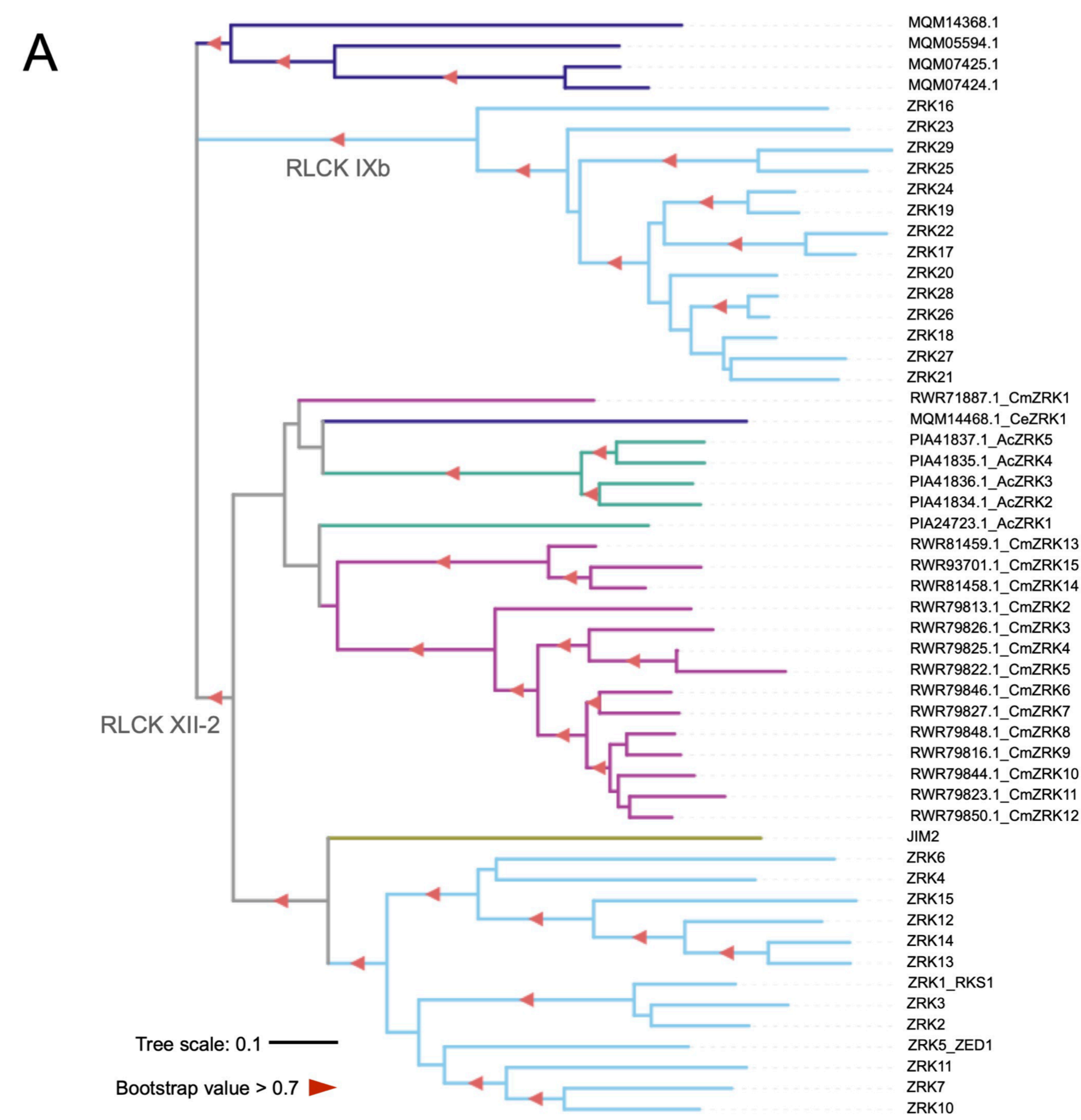

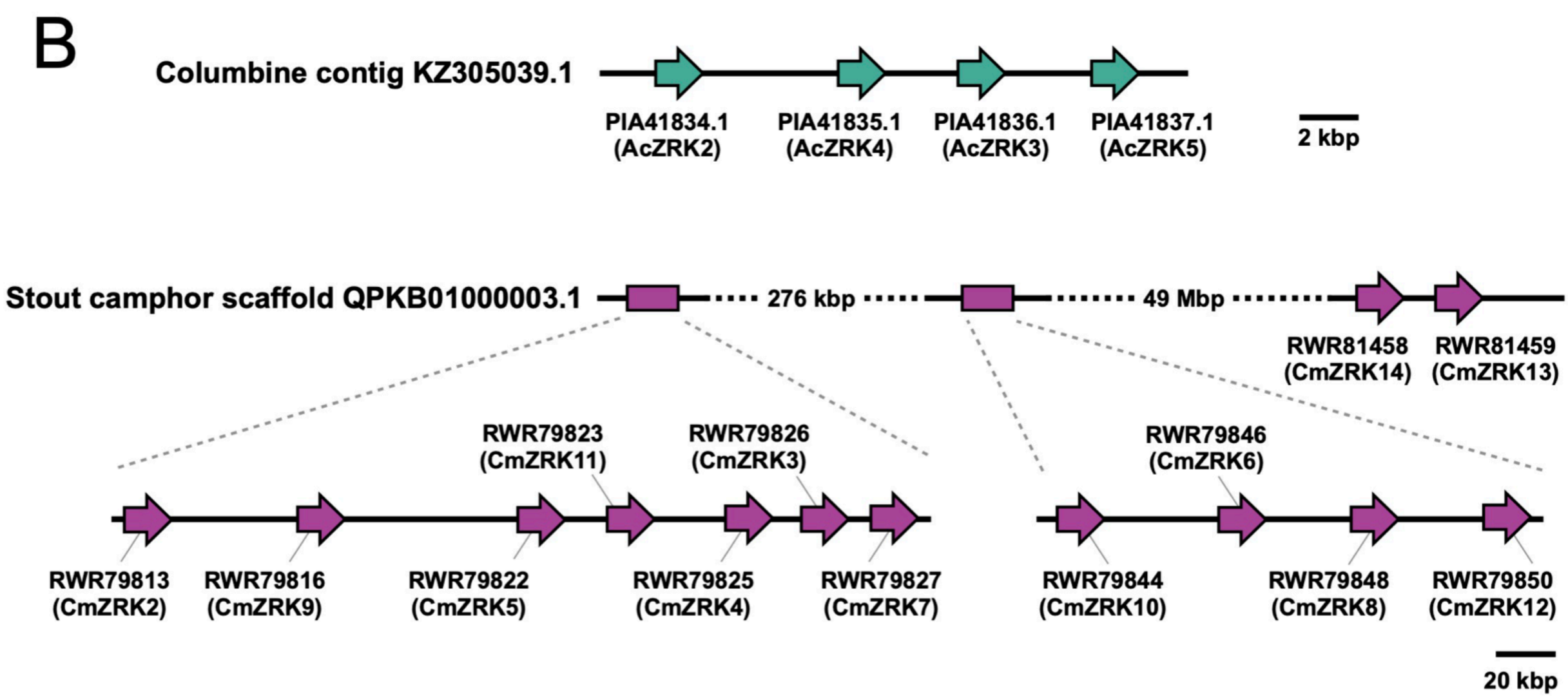

Figure 5. ZRK gene clusters occur in *Aquilegia coerulea* and *Cinnamomum micranthum*. (**A**) The phylogenetic tree was generated in MEGA7 by the neighbor-joining method using full length amino acid sequences of 39 ZRK proteins. Each branch is marked with different colors based on the plant taxonomy. Red triangles indicate bootstrap support > 0.7. The scale bar indicates the evolutionary distance in amino acid substitution per site. (**B**) Schematic representation of the ZRK gene clusters on an *A. coerulea* (columbine) contig and a *C. micranthum* (stout camphor) scaffold.

Figure 6. ZRK family proteins positively regulate *Aquilegia coerulea* AcZAR1 and *Cinnamomum micranthum* CmZAR1 autoimmune cell death in *Nicotiana benthamiana*. (**A, C**) Cell death observed in *N. benthamiana* after expression of ZAR1 mutants with or without wild-type ZRKs. *N. benthamiana* leaf panels expressing wild-type NbZAR1 ($NbZAR1^{WT}$), $NbZAR1^{D481V}$ ($ZAR1^{D481V}$), $AcZAR1^{D489V}$ ($AcZAR1^{DV}$) and $CmZAR1^{D488V}$ ($CmZAR1^{DV}$) with or without wild-type ZRKs, were photographed at four days after agroinfiltration. (**B, D**) Violin plots show AcZAR1 and CmZAR1 cell death intensity scored as an HR index based on 12 and nine replicates (different leaves from independent plants) in two independent experiments. Different colors of plots describe data from different experiments. Statistical differences among the samples were analyzed with Tukey's HSD test ($p<0.01$).

A

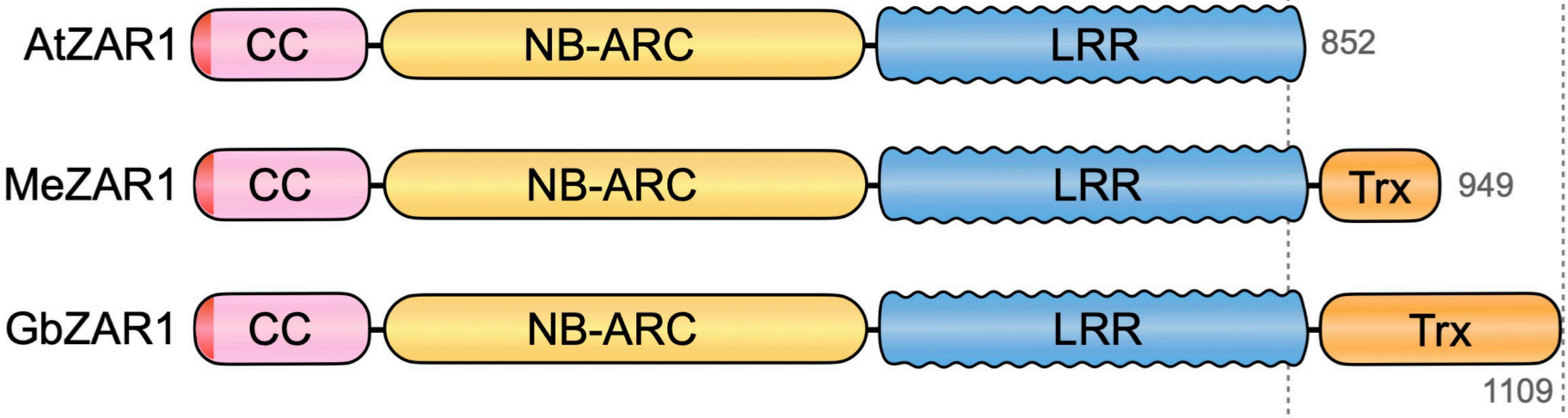

B

```
AtZAR1  ESFAIEDVGFRGGVWMK----------------------------------
MeZAR1  TSFPIEDIGFRGGVWTKGEHKA-----------------------------
GbZAR1  VSFPIDDVGFRGGMRAGNERISIEAWNYKGLNLGLVELILACGLLGPKEREMDPDSVKST

AtZAR1  ----------------------------------------------------
MeZAR1  ----------------NKELIAQEKSQTSSSINQEVDLDVLMD----------------
GbZAR1  LSNLAFGNVMAAAARDYQKELLAQEKAQ-SSTANEEVDLDELMDDPELEKLHADRIAALK

AtZAR1  ----------------------------------------------------
MeZAR1  KEAEKRETLKKQGHGEYREIAEGDFLGEVTGSEKVICHFYHREFYRCKYSYCFNSLFHSL
GbZAR1  KEAEKREALKRKGHGDYREITEGDFLGEVTGSEKVVCHFYHKEFYRCK---IMDKHLKAL

AtZAR1  ----------------------TPL----------------------------
MeZAR1  GRALLNI----------FYITNF----MSC----------------------------
GbZAR1  ALKHMDTKFIKLDAENAPFFVTKLAVKTLPCVIIFRKGVAVDRLVGFQDLGAKDDFAMRT

AtZAR1  ----------------------------HRT-----------
MeZAR1  ----------------------------------------
GbZAR1  LEVVLIKKGIISEKKNEDDEDDVYDESRHRTVRSSVNHDSDSD
```

Figure 7. Cassava and cotton ZAR1-ID carry an additional Trx domain at the C terminus. (**A**) Schematic representation of NLR domain architecture with C-terminal Trx domain. (**B**) Description of Trx domain sequences on amino acid sequence alignment. Cassava XP_021604862.1 (MeZAR1) and cotton KAB1998109.1 (GbZAR1) were used for MAFFT version 7 alignment as representative ZAR1-ID. Arabidopsis ZAR1 (AtZAR1) was used as a control of ZAR1 without ID.

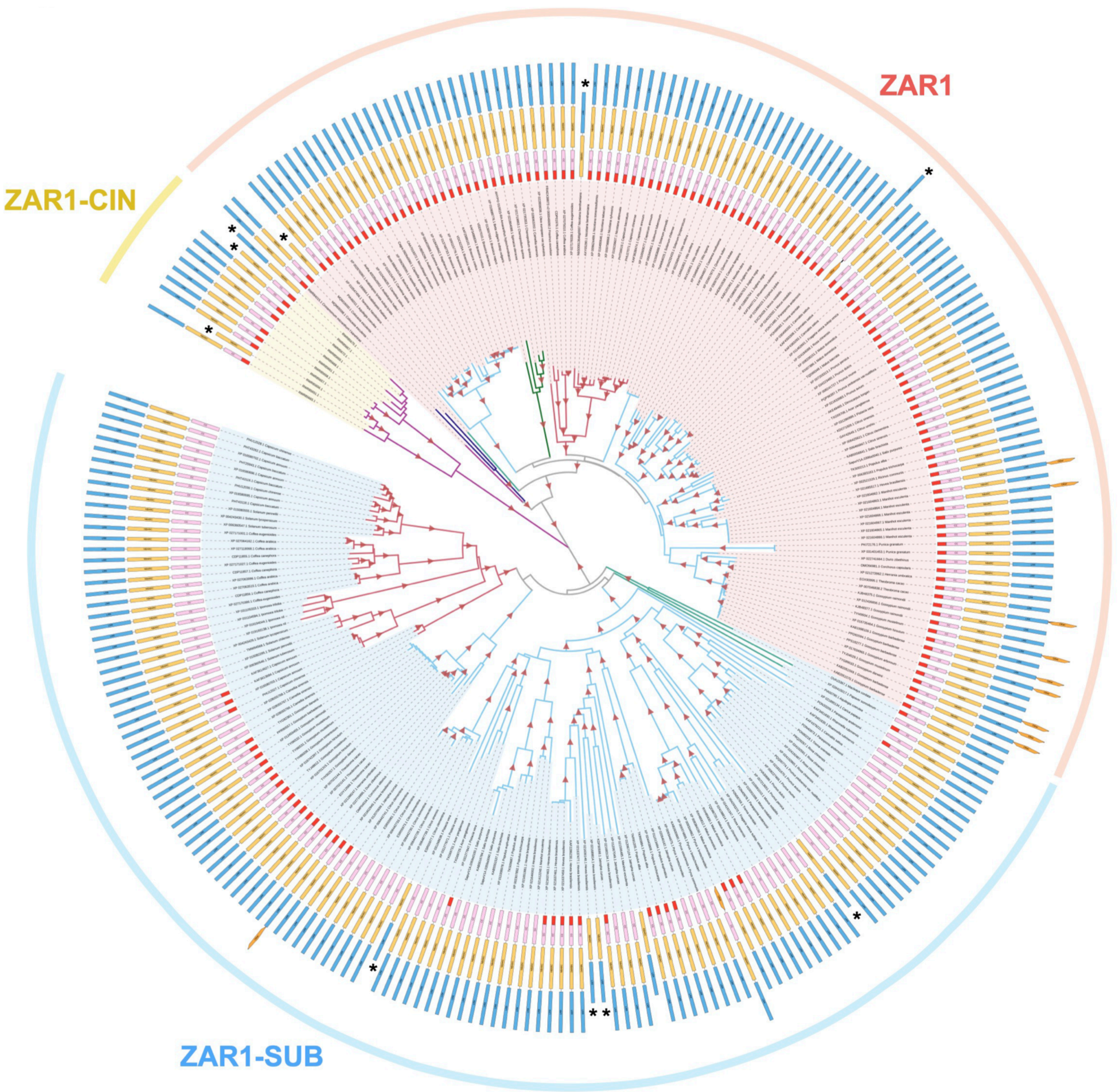

Figure 8. ZAR1-SUB has emerged early in eudicots and diverged at MADA motif sequence. The phylogenetic tree was generated in MEGA7 by the neighbor-joining method using full length amino acid sequences of 120 ZAR1, 129 ZAR1-SUB and 11 ZAR1-CIN identified in Figure 1. Each branch is marked with different colors based on the plant taxonomy. Red triangles indicate bootstrap support > 0.7. The scale bar indicates the evolutionary distance in amino acid substitution per site. NLR domain architectures are illustrated outside of the leaf labels: MADA is red, CC is pink, NB-ARC is yellow, LRR is blue and other domain is orange. Black asterisks on domain schemes describe truncated NLRs or potentially mis-annotated NLR.

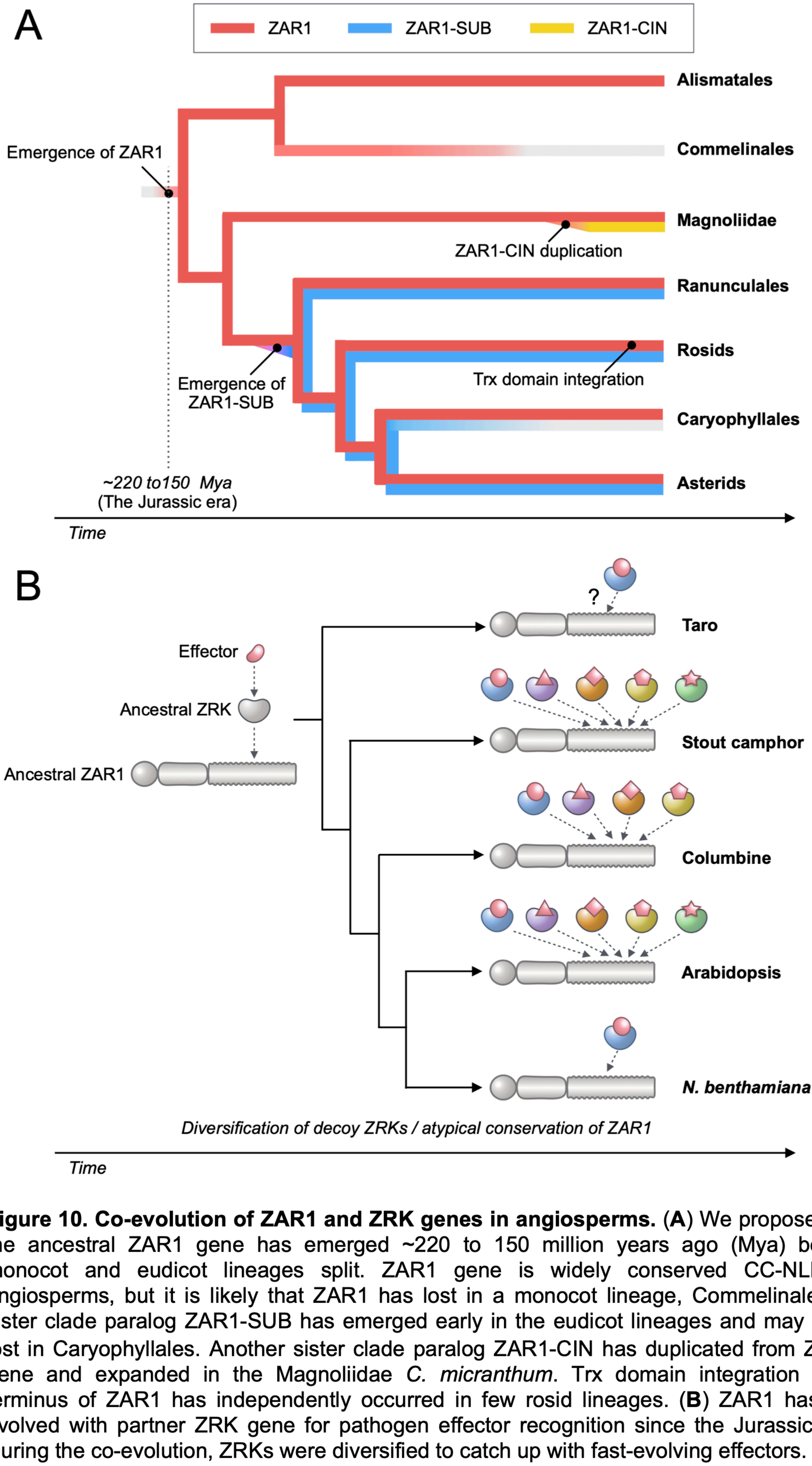

Figure 10. Co-evolution of ZAR1 and ZRK genes in angiosperms. (**A**) We propose that the ancestral ZAR1 gene has emerged ~220 to 150 million years ago (Mya) before monocot and eudicot lineages split. ZAR1 gene is widely conserved CC-NLR in angiosperms, but it is likely that ZAR1 has lost in a monocot lineage, Commelinales. A sister clade paralog ZAR1-SUB has emerged early in the eudicot lineages and may have lost in Caryophyllales. Another sister clade paralog ZAR1-CIN has duplicated from ZAR1 gene and expanded in the Magnoliidae *C. micranthum*. Trx domain integration to C terminus of ZAR1 has independently occurred in few rosid lineages. (**B**) ZAR1 has co-evolved with partner ZRK gene for pathogen effector recognition since the Jurassic era. During the co-evolution, ZRKs were diversified to catch up with fast-evolving effectors.

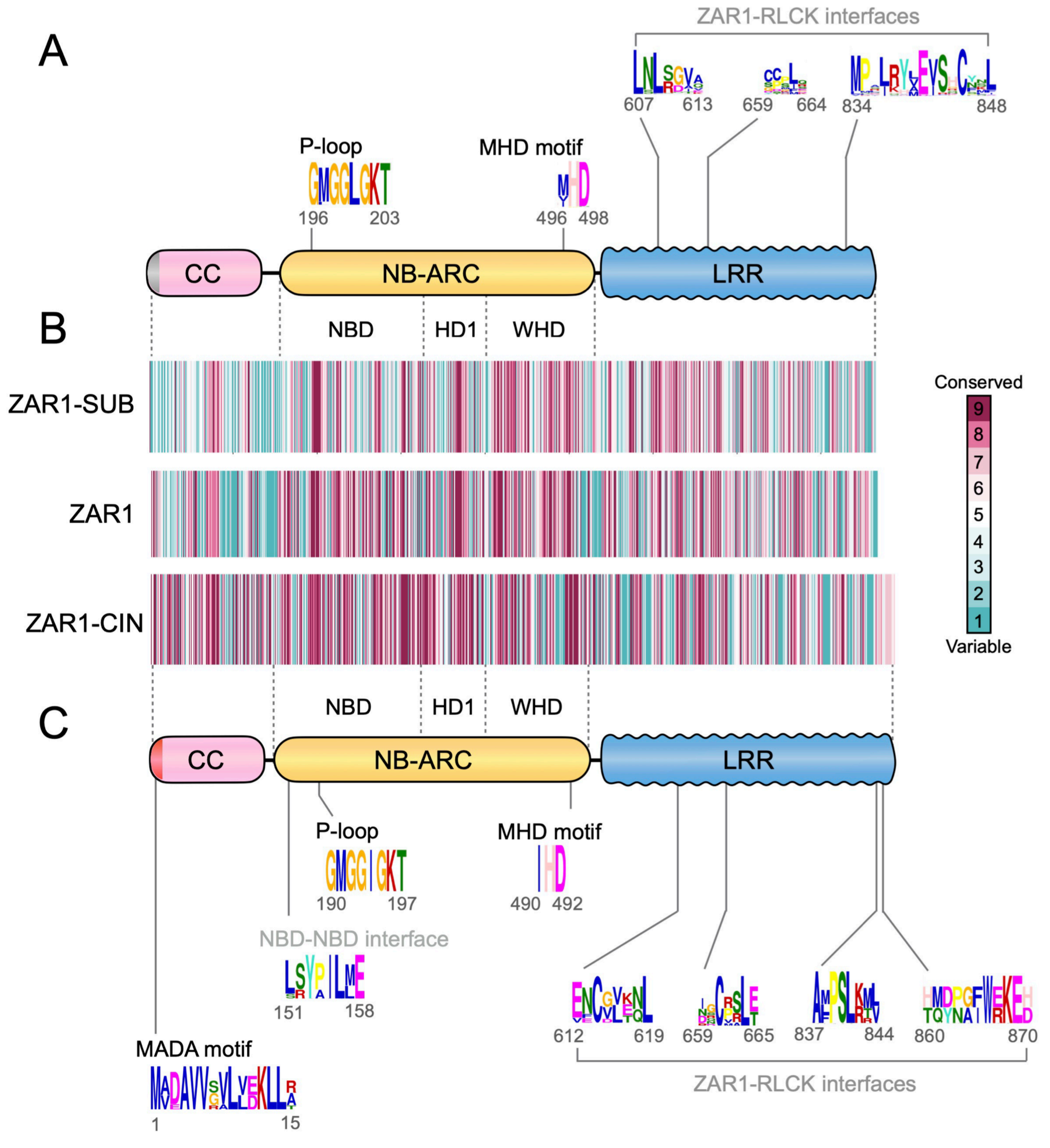

Figure 9. Conserved sequence distributions in ZAR1-SUB and ZAR1-CIN. (**A**) Schematic representation of the ZAR1-SUB protein highlighting the position of the representative conserved sequence patterns across ZAR1-SUB. Representative consensus sequence patterns identified by MEME are described on the scheme. Raw MEME motifs are listed in Supplemental Tables 2 and 3. (**B**) Conservation and variation of each amino acid among ZAR1-SUB and ZAR1-CIN. Amino acid alignment of 129 ZAR1-SUB or 8 ZAR1-CIN was used for conservation score calculation via the ConSurf server (https://consurf.tau.ac.il). The conservation scores are mapped onto each amino acid position in queries XP_004243429.1 (ZAR1-SUB) and RWR85656.1 (ZAR1-CIN), respectively. (**C**) Schematic representation of the ZAR1-CIN protein highlighting the position of the representative conserved sequence patterns across 8 ZAR1-CIN. Raw MEME motifs are listed in Supplemental Tables 4 and 5.

Parsed Citations

Adachi H, Derevnina L, Kamoun S. (2019a) NLR singletons, pairs, and networks: evolution, assembly, and regulation of the intracellular immunoreceptor circuitry of plants. Curr Opin Plant Biol 50:121-131. doi:10.1016/j.pbi.2019.04.007.

Adachi H, Contreras MP, Harant A, Wu CH, Derevnina L, Sakai T, Duggan C, Moratto E, Bozkurt TO, Maqbool A, Win J, Kamoun S. (2019b) An N-terminal motif in NLR immune receptors is functionally conserved across distantly related plant species. eLife 8: e49956. doi: 10.7554/eLife.49956.
Google Scholar: Author Only Title Only Author and Title

Adachi H, Sakai T, Kourelis J, Maqbool A, Kamoun S. (2020) Jurassic NLR: conserved and dynamic evolutionary features of the atypically ancient immune receptor ZAR1. bioRxiv doi: https://doi.org/10.1101/2020.10.12.333484
Google Scholar: Author Only Title Only Author and Title

Altschul SF, Gish W, Miller W, Myers EW, Lipman DJ. (1990) Basic local alignment search tool. J Mol Biol 215: 403-10. doi: 10.1016/S0022-2836(05)80360-2.
Google Scholar: Author Only Title Only Author and Title

Ashkenazy H, Abadi S, Martz E, et al. (2016) ConSurf 2016: an improved methodology to estimate and visualize evolutionary conservation in macromolecules. Nucleic Acids Res 44: W344-W350. doi:10.1093/nar/gkw408.
Google Scholar: Author Only Title Only Author and Title

Baggs E, Dagdas G, Krasileva KV. (2017) NLR diversity, helpers and integrated domains: making sense of the NLR IDentity. Curr Opin Plant Biol 38: 59-67. doi:10.1016/j.pbi.2017.04.012.
Google Scholar: Author Only Title Only Author and Title

Bailey TL, Elkan C. (1994) Fitting a mixture model by expectation maximization to discover motifs in biopolymers. Proc Int Conf Intell Syst Mol Biol 2:28-36.
Google Scholar: Author Only Title Only Author and Title

Baudin M, Hassan JA, Schreiber KJ, Lewis JD. (2017) Analysis of the ZAR1 immune complex reveals determinants for immunity and molecular interactions. Plant Physiol 174: 2038-2053. doi: 10.1104/pp.17.00441.
Google Scholar: Author Only Title Only Author and Title

Baudin M, Schreiber KJ, Martin EC, Petrescu AJ, Lewis JD. (2019) Structure-function analysis of ZAR1 immune receptor reveals key molecular interactions for activity. Plant J 101: 352-370. doi: 10.1111/tpj.14547.
Google Scholar: Author Only Title Only Author and Title

Bayless AM, Nishimura MT. (2020) Enzymatic functions for Toll/Interleukin-1 receptor domain proteins in the plant immune system. Front Genet 11:539. doi:10.3389/fgene.2020.00539.
Google Scholar: Author Only Title Only Author and Title

Bentham AR, Zdrzalek R, De la Concepcion JC, Banfield MJ. (2018) Uncoiling CNLs: structure/Function approaches to understanding CC domain function in plant NLRs. Plant and Cell Physiology 59:2398–2408. doi: https://doi.org/10.1093/pcp/pcy185.
Google Scholar: Author Only Title Only Author and Title

Benson DA, Cavanaugh M, Clark K, Karsch-Mizrachi I, Lipman DJ, Ostell J, Sayers EW. (2013) GenBank. Nucleic Acids Res 41: D36-42. doi: 10.1093/nar/gks1195.
Google Scholar: Author Only Title Only Author and Title

Bi G, Su M, Li N, et al. (2021) The ZAR1 resistosome is a calcium-permeable channel triggering plant immune signaling. Cell 184:3528-3541.e12. doi: 10.1016/j.cell.2021.05.003.
Google Scholar: Author Only Title Only Author and Title

Bos JI, Kanneganti TD, Young C, Cakir C, Huitema E, Win J, Armstrong MR, Birch PR, Kamoun S. (2006) The C-terminal half of Phytophthora infestans RXLR effector AVR3a is sufficient to trigger R3a-mediated hypersensitivity and suppress INF1- induced cell death in Nicotiana benthamiana. Plant J 48: 165-176. doi: 10.1111/j.1365-313X.2006.02866.x.
Google Scholar: Author Only Title Only Author and Title

Boutrot F, Zipfel C. (2017) Function, discovery, and exploitation of plant pattern recognition receptors for broad-spectrum disease resistance. Annu Rev Phytopathol 55: 257-286. doi:10.1146/annurev-phyto-080614-120106.
Google Scholar: Author Only Title Only Author and Title

Burdett H, Bentham AR, Williams SJ, et al. (2019) The plant "resistosome": structural insights into immune signaling. Cell Host Microbe 26:193-201. doi:10.1016/j.chom.2019.07.020.
Google Scholar: Author Only Title Only Author and Title

Cesari S, Bernoux M, Moncuquet P, Kroj T, Dodds PN. (2014) A novel conserved mechanism for plant NLR protein pairs: the "integrated decoy" hypothesis. Front Plant Sci 5:606. doi:10.3389/fpls.2014.00606.
Google Scholar: Author Only Title Only Author and Title

Chaw SM, Liu YC, Wu YW, et al. (2019) Stout camphor tree genome fills gaps in understanding of flowering plant genome evolution. Nat Plants 5:63-73. doi:10.1038/s41477-018-0337-0.
Google Scholar: Author Only Title Only Author and Title

Chen S, Zhou Y, Chen Y, Gu J. (2018) fastp: an ultra-fast all-in-one FASTQ preprocessor. Bioinformatics 34: i884-i890. doi: 10.1093/bioinformatics/bty560.
Google Scholar: Author Only Title Only Author and Title

Coiro M, Doyle JA, Hilton J. (2019) How deep is the conflict between molecular and fossil evidence on the age of angiosperms? New Phytol 223: 83-99. doi: 10.1111/nph.15708.
Google Scholar: Author Only Title Only Author and Title

Cui D-F, Hou Y, Yin P, Wang X. (2022) A Jurassic flower bud from China. Geological Society, London 521:81-93. https://doi.org/10.1144/SP521-2021-122
Google Scholar: Author Only Title Only Author and Title

Dangl JL, Horvath DM, Staskawicz BJ. (2013) Pivoting the plant immune system from dissection to deployment. Science 341:746-751. doi:10.1126/science.1236011.
Google Scholar: Author Only Title Only Author and Title

Delaux PM, Hetherington AJ, Coudert Y, et al. (2019) Reconstructing trait evolution in plant evo-devo studies. Curr Biol 29:R1110-R1118. doi:10.1016/j.cub.2019.09.044.
Google Scholar: Author Only Title Only Author and Title

Dodds PN, Rathjen JP. (2010) Plant immunity: towards an integrated view of plant-pathogen interactions. Nat Rev Genet 11:539-548. doi:10.1038/nrg2812.
Google Scholar: Author Only Title Only Author and Title

Duxbury Z, Wang S, MacKenzie CI, et al. (2020) Induced proximity of a TIR signaling domain on a plant-mammalian NLR chimera activates defense in plants. Proc Natl Acad Sci U S A 117: 18832-18839. doi:10.1073/pnas.2001185117.
Google Scholar: Author Only Title Only Author and Title

Eddy SR. (1998) Profile hidden markov models. Bioinformatics 14:755-763. DOI: https://doi.org/10.1093/ bioinformatics/14.9.755.
Google Scholar: Author Only Title Only Author and Title

Engler C, Youles M, Gruetzner R, Ehnert TM, Werner S, Jones JD, Patron NJ, Marillonnet S. (2014) A golden gate modular cloning toolbox for plants. ACS Synth Biol 3: 839-843. doi: 10.1021/sb4001504.
Google Scholar: Author Only Title Only Author and Title

Feehan JM, Castel B, Bentham AR, Jones JD. (2020) Plant NLRs get by with a little help from their friends. Curr Opin Plant Biol 56:99-108. doi:10.1016/j.pbi.2020.04.006.
Google Scholar: Author Only Title Only Author and Title

Filiault DL, Ballerini ES, Mandáková T, et al. (2018) The Aquilegia genome provides insight into adaptive radiation and reveals an extraordinarily polymorphic chromosome with a unique history. ELife 7:e36426. doi: 10.7554/eLife.36426.
Google Scholar: Author Only Title Only Author and Title

Fu Q, Diez JB, Pole M, et al. (2018) An unexpected noncarpellate epigynous flower from the Jurassic of China. Elife 7: e38827. doi:10.7554/eLife.38827.
Google Scholar: Author Only Title Only Author and Title

Gong Z, Qi J, Hu M, Bi G, Zhou JM, Han GZ. (2022) The origin and evolution of a plant resistosome. Plant Cell 34: 1600-1620. doi:10.1093/plcell/koac053.
Google Scholar: Author Only Title Only Author and Title

Goodstein DM, Shu S, Howson R, Neupane R, Hayes RD, Fazo J, Mitros T, Dirks W, Hellsten U, Putnam N, Rokhsar DS. (2012) Phytozome: a comparative platform for green plant genomics. Nucleic Acids Res 40: D1178-1186. doi: 10.1093/nar/gkr944.
Google Scholar: Author Only Title Only Author and Title

Harant A, Pai H, Sakai T, Kamoun S, Adachi H. (2022) A vector system for fast-forward studies of the HOPZ-ACTIVATED RESISTANCE1 (ZAR1) resistosome in the model plant Nicotiana benthamiana. Plant Physiol. 188: 70-80. doi: 10.1093/plphys/kiab471.
Google Scholar: Author Only Title Only Author and Title

Hu M, Qi J, Bi G, Zhou JM. (2020) Bacterial effectors induce oligomerization of immune receptor ZAR1 in vivo. Mol Plant pii: S1674-2052(20)30066-6. doi: 10.1016/j.molp.2020.03.004.
Google Scholar: Author Only Title Only Author and Title

Jacob P, Kim NH, Wu F, et al. (2021) The plant immune receptors NRG1.1 and ADR1 are calcium influx channels. bioRxiv doi: https://doi.org/10.1101/2021.02.25.431980.

Google Scholar: Author Only Title Only Author and Title

Jones JD, Dangl JL. (2006) The plant immune system. Nature 444: 323-329. doi:10.1038/nature05286.
Google Scholar: Author Only Title Only Author and Title

Jones JD, Vance RE, Dangl JL. (2016) Intracellular innate immune surveillance devices in plants and animals. Science 354: aaf6395. doi:10.1126/science.aaf6395.
Google Scholar: Author Only Title Only Author and Title

Jones P, Binns D, Chang H, Fraser M, Li W, McAnulla C, McWilliam H, Maslen J, Mitchell A, Nuka G, Pesseat S, Quinn A, Sangrador-Vegas A, Scheremetjew M, Yong S, Lopez R, Hunter S. (2014) InterProScan 5: genome-scale protein function classification. Bioinformatics 30: 1236-1240. doi: 10.1093/bioinformatics/btu031.
Google Scholar: Author Only Title Only Author and Title

Jubic LM, Saile S, Furzer OJ, El Kasmi F, Dangl JL. (2019) Help wanted: helper NLRs and plant immune responses. Curr Opin Plant Biol 50: 82-94. doi:10.1016/j.pbi.2019.03.013.
Google Scholar: Author Only Title Only Author and Title

Karasov TL, Chae E, Herman JJ, Bergelson J. (2017) Mechanisms to mitigate the trade-off between growth and defense. Plant Cell 29: 666-680. doi:10.1105/tpc.16.00931.
Google Scholar: Author Only Title Only Author and Title

Katoh K, Standley DM. (2013) MAFFT multiple sequence alignment software version 7: improvements in performance and usability. Mol Biol Evol 30: 772-780. doi: 10.1093/molbev/mst010.
Google Scholar: Author Only Title Only Author and Title

Kelley LA, Mezulis S, Yates CM, Wass MN, Sternberg MJ. (2015) The Phyre2 web portal for protein modeling, prediction and analysis. Nat Protoc 10: 845-858. doi: 10.1038/nprot.2015.053.
Google Scholar: Author Only Title Only Author and Title

Kourelis J, van der Hoorn RAL. (2018) Defended to the nines: 25 years of resistance gene cloning identifies nine mechanisms for R protein function. The Plant Cell 30: 285-299. doi: https://doi.org/10.1105/tpc.17.00579.
Google Scholar: Author Only Title Only Author and Title

Kourelis J, Sakai T, Adachi H, Kamoun S. (2021) RefPlantNLR is a comprehensive collection of experimentally validated plant disease resistance proteins from the NLR family. PLoS Biol 19:e3001124. doi: 10.1371/journal.pbio.3001124.
Google Scholar: Author Only Title Only Author and Title

Kroj T, Chanclud E, Michel-Romiti C, Grand X, Morel JB. (2016) Integration of decoy domains derived from protein targets of pathogen effectors into plant immune receptors is widespread. New Phytol 210: 618-626. doi:10.1111/nph.13869.
Google Scholar: Author Only Title Only Author and Title

Kumar S, Stecher G, Tamura K. (2016) MEGA7: Molecular Evolutionary Genetics Analysis Version 7.0 for Bigger Datasets. Mol Biol Evol 33: 1870-1874. doi: 10.1093/molbev/msw054.
Google Scholar: Author Only Title Only Author and Title

Laflamme B, Dillon MM, Martel A, Almeida RND, Desveaux D, Guttman DS. (2020) The pan-genome effector-triggered immunity landscape of a host-pathogen interaction. Science 367: 763-768. doi:10.1126/science.aax4079.
Google Scholar: Author Only Title Only Author and Title

Lee H-Y, Mang H, Choi E-H, Seo Y-E, Kim M-S, Oh S, Kim S-B, Choi D. (2020) Genome-wide functional analysis of hot pepper immune receptors reveals an autonomous NLR cluster in seed plants. bioRxiv doi: https://doi.org/10.1101/2019.12.16.878959.
Google Scholar: Author Only Title Only Author and Title

Lee RRQ, Chae E. (2020) Variation patterns of NLR clusters in Arabidopsis thaliana genomes. Plant Communications https://doi.org/10.1016/j.xplc.2020.100089.
Google Scholar: Author Only Title Only Author and Title

Lewis JD, Wu R, Guttman DS, Desveaux D. (2010) Allele-specific virulence attenuation of the Pseudomonas syringae HopZ1a type III effector via the Arabidopsis ZAR1 resistance protein. PLoS Genet 6: e1000894. doi: 10.1371/journal.pgen.1000894.
Google Scholar: Author Only Title Only Author and Title

Lewis JD, Lee AH, Hassan JA, et al. (2013) The Arabidopsis ZED1 pseudokinase is required for ZAR1-mediated immunity induced by the Pseudomonas syringae type III effector HopZ1a. Proc Natl Acad Sci U S A. 110: 18722-18727. doi:10.1073/pnas.1315520110.
Google Scholar: Author Only Title Only Author and Title

Li, Bo, Ruotti, Victor, Stewart, Ron M., Thomson, James A., Dewey, Colin N. (2010) RNA-Seq gene expression estimation with read mapping uncertainty. Bioinformatics 26: 493-500. doi:10.1093/bioinformatics/btp692.
Google Scholar: Author Only Title Only Author and Title

Liang X, Zhou JM. (2018) Receptor-like cytoplasmic kinases: central players in plant receptor kinase-mediated signaling. Annu

Rev Plant Biol 69: 267-299. doi:10.1146/annurev-arplant-042817-040540.
Google Scholar: Author Only Title Only Author and Title

Lin X, Zhang Y, Kuang H, Chen J. (2013) Frequent loss of lineages and deficient duplications accounted for low copy number of disease resistance genes in Cucurbitaceae. BMC Genomics 14: 335. doi:10.1186/1471-2164-14-335.
Google Scholar: Author Only Title Only Author and Title

Ma S, Lapin D, Liu L, et al. (2020) Direct pathogen-induced assembly of an NLR immune receptor complex to form a holoenzyme. Science 370: eabe3069. doi: 10.1126/science.abe3069.
Google Scholar: Author Only Title Only Author and Title

Martin R, Qi T, Zhang H, Liu F, King M, Toth C, Nogales E, Staskawicz BJ. (2020) Structure of the activated ROQ1 resistosome directly recognizing the pathogen effector XopQ. Science 370: eabd9993. doi: 10.1126/science.abd9993.
Google Scholar: Author Only Title Only Author and Title

Mermigka G, Amprazi M, Mentzelopoulou A, Amartolou A, Sarris PF. (2020) Plant and animal innate immunity complexes: fighting different enemies with similar weapons. Trends Plant Sci 25: 80-91. doi:10.1016/j.tplants.2019.09.008.
Google Scholar: Author Only Title Only Author and Title

Michelmore RW, Meyers BC. (1998) Clusters of resistance genes in plants evolve by divergent selection and a birth-and-death process. Genome Res 8: 1113-1130. doi:10.1101/gr.8.11.1113.
Google Scholar: Author Only Title Only Author and Title

Pai H, Kourelis J, Adachi H, Kamoun S (2023) ZED1-related kinases (ZRKs) from Aquilegia coerulea and Cinnamomum micranthum do not trigger autoactive cell death in Nicotiana benthamiana. Zenodo https://doi.org/10.5281/zenodo.7844723.
Google Scholar: Author Only Title Only Author and Title

Prigozhin DM, Krasileva KV. (2020) Intraspecies diversity reveals a subset of highly variable plant immune receptors and predicts their binding sites. bioRxiv doi: https://doi.org/10.1101/2020.07.10.190785.
Google Scholar: Author Only Title Only Author and Title

Robinson JT, Thorvaldsdóttir H, Winckler W, Guttman M, Lander ES, Getz G, Mesirov JP. (2011) Integrative genomics viewer. Nat Biotechnol 29: 24-26. doi: 10.1038/nbt.1754.
Google Scholar: Author Only Title Only Author and Title

Sarris PF, Cevik V, Dagdas G, Jones JD, Krasileva KV. (2016) Comparative analysis of plant immune receptor architectures uncovers host proteins likely targeted by pathogens. BMC Biol 14: 8. doi:10.1186/s12915-016-0228-7.
Google Scholar: Author Only Title Only Author and Title

Seong K, Seo E, Witek K, Li M, Staskawicz B. (2020) Evolution of NLR resistance genes with noncanonical N-terminal domains in wild tomato species. New Phytol 227: 1530-1543. doi:10.1111/nph.16628.
Google Scholar: Author Only Title Only Author and Title

Seto D, Koulena N, Lo T, Menna A, Guttman DS, Desveaux D. (2017) Expanded type III effector recognition by the ZAR1 NLR protein using ZED1-related kinases. Nat Plants 3: 17027. doi:10.1038/nplants.2017.27.
Google Scholar: Author Only Title Only Author and Title

Schultink A, Qi T, Bally J, Staskawicz B. (2019) Using forward genetics in Nicotiana benthamiana to uncover the immune signaling pathway mediating recognition of the Xanthomonas perforans Effector XopJ4. New Phytol 221: 1001-1009. doi: 10.1111/nph.15411.
Google Scholar: Author Only Title Only Author and Title

Smith SA, Brown JW. (2018) Constructing a broadly inclusive seed plant phylogeny. Am J Bot 105: 302-314. doi:10.1002/ajb2.1019.
Google Scholar: Author Only Title Only Author and Title

Shao ZQ, Xue JY, Wu P, et al. (2016) Large-scale analyses of angiosperm nucleotide-binding site-leucine-rich repeat genes reveal three anciently diverged classes with distinct evolutionary patterns. Plant Physiol 170: 2095-2109. doi:10.1104/pp.15.01487.
Google Scholar: Author Only Title Only Author and Title

Stam R, Silva-Arias GA, Tellier A. (2019) Subsets of NLR genes show differential signatures of adaptation during colonization of new habitats. New Phytol 224: 367-379. doi:10.1111/nph.16017.
Google Scholar: Author Only Title Only Author and Title

Steuernagel B, Jupe F, Witek K, Jones JD, Wulff BB. (2015) NLR-parser: rapid annotation of plant NLR complements. Bioinformatics 31: 1665-1667. doi: 10.1093/bioinformatics/btv005.
Google Scholar: Author Only Title Only Author and Title

Sukumaran J, Holder MT. (2010) DendroPy: a Python library for phylogenetic computing. Bioinformatics 26: 1569-1571. doi: 10.1093/bioinformatics/btq228.
Google Scholar: Author Only Title Only Author and Title

Tamborski J, Krasileva KV. (2020) Evolution of plant NLRs: from natural history to precise modifications. Annu Rev Plant Biol 71:

355-378. doi:10.1146/annurev-arplant-081519-035901.
Google Scholar: Author Only Title Only Author and Title

Uehling J, Deveau A, Paoletti M. (2017) Do fungi have an innate immune response? An NLR-based comparison to plant and animal immune systems. PLoS Pathog 13: e1006578. doi:10.1371/journal.ppat.1006578.
Google Scholar: Author Only Title Only Author and Title

Van de Weyer AL, Monteiro F, Furzer OJ, et al. (2019) A species-wide inventory of NLR genes and alleles in Arabidopsis thaliana. Cell 178: 1260-1272.e14. doi:10.1016/j.cell.2019.07.038.
Google Scholar: Author Only Title Only Author and Title

Wang G, Roux B, Feng F, et al. (2015) The decoy substrate of a pathogen effector and a pseudokinase specify pathogen-induced modified-self recognition and immunity in plants. Cell Host Microbe 18: 285-295. doi:10.1016/j.chom.2015.08.004.
Google Scholar: Author Only Title Only Author and Title

Wang J, Wang J, Hu M, W Shan, Qi J, Wang G, Han Z, Qi Y, Gao N, Wang H-W, Zhou J-M, Chai J. (2019a) Ligand-triggered allosteric ADP release primes a plant NLR complex. Science 364: eaav5868. doi: 10.1126/science.aav5868.
Google Scholar: Author Only Title Only Author and Title

Wang J, Hu M, Wang J, Qi J, Han Z, Wang G, Qi Y, Wang H-W, Zhou J-M, Chai J. (2019b) Reconstitution and structure of a plant NLR resistosome conferring immunity. Science 364: eaav5870. doi: 10.1126/science.aav5870.
Google Scholar: Author Only Title Only Author and Title

Wang J, Chai J. (2020) Structural Insights into the Plant Immune Receptors PRRs and NLRs. Plant Physiol 182: 1566-1581. doi:10.1104/pp.19.01252.
Google Scholar: Author Only Title Only Author and Title

Weber E, Engler C, Gruetzner R, Werner S, Marillonnet S. (2011) A modular cloning system for standardized assembly of multigene constructs. PLoS One 6: e16765. doi: 10.1371/journal.pone.0016765.
Google Scholar: Author Only Title Only Author and Title

Wu CH, Krasileva KV, Banfield MJ, Terauchi R, Kamoun S. (2015) The "sensor domains" of plant NLR proteins: more than decoys? Front Plant Sci 6: 134. doi:10.3389/fpls.2015.00134.
Google Scholar: Author Only Title Only Author and Title

Wu CH, Abd-El-Haliem A, Bozkurt TO, et al. (2017) NLR network mediates immunity to diverse plant pathogens. Proc Natl Acad Sci U S A 114: 8113-8118. doi:10.1073/pnas.1702041114.
Google Scholar: Author Only Title Only Author and Title

Wu CH, Derevnina L, Kamoun S. (2018) Receptor networks underpin plant immunity. Science 360: 1300-1301. doi:10.1126/science.aat2623.
Google Scholar: Author Only Title Only Author and Title

Xiong Y, Han Z, Chai J. (2020) Resistosome and inflammasome: platforms mediating innate immunity. Curr Opin Plant Biol 56: 47-55. doi:10.1016/j.pbi.2020.03.010.
Google Scholar: Author Only Title Only Author and Title

Zhou JM, Zhang Y. (2020) Plant immunity: danger perception and signaling. Cell 181: 978-989. doi:10.1016/j.cell.2020.04.028.
Google Scholar: Author Only Title Only Author and Title